PCA

Open File Report 89-48

IMPLEMENTATION OF AN INTEGRATED ROCK MECHANICS PROGRAMME FOR CUT AND FILL POTASH MINING

by

R.J. Beddoes, J.J. Streisel, and B.V. Roulston
Potash Company of America, Division of Rio Algom Ltd.

Canada-New Brunswick Mineral Development Agreement
Entente Canada-Nouveau-Brunswick L'Exploitation Minérale

Natural Resources and Energy New Brunswick
Ressources Naturelles et Énergie Nouveau-Brunswick
Energy, Mines and Resources Canada
Énergie, Mines et Ressources Canada

Price $4.40

This report has been prepared for:

Minerals and Energy Division
Department of Natural Resources and Energy
New Brunswick

Hon. Morris Green, Minister

November, 1989

IMPLEMENTATION OF AN INTEGRATED ROCK MECHANICS PROGRAMME FOR CUT AND FILL POTASH MINING

This project was funded under the Canada-New Brunswick Mineral Development Agreement, a subsidiary agreement under the Economic and Regional Development Agreement.

Copies available by contacting:

Minerals and Energy Division
Department of Natural Resources and Energy
P.O. Box 6000, Fredericton
New Brunswick E3B 5H1

November, 1989

Report No.: Open File Report 89-48

Authors: R.J. Beddoes, J.J. Streisel and B.V. Roulston,
Potash Company of America,
Division of Rio Algom Ltd.

Catalogue No.: ISSN 0712-4562

This report should be referenced in the following manner:

BEDDOES, R.J., STREISEL, J.J., and ROULSTON, B.V. 1989. Implementation of an integrated rock mechanics programme for cut and fill potash mining. New Brunswick Department of Natural Resources and Energy, Minerals and Energy Division, Open File Report 89-48, 76 p.

Implementation of an Integrated Rock Mechanics Programme for Cut and Fill Potash Mining

R. J. Beddoes
J. J. Streisel
B. V. Roulston

Potash Company of America, Division of Rio Algom Ltd.
Sussex, New Brunswick

July, 1989

90-01600/

Funding for this study was provided in part by the New Brunswick Department of Natural Resources and Energy under the Canada/New Brunswick Mineral Development Agreement.

Abstract

Unique rock mechanics problems are presented by the steeply dipping and contorted potash ore body mined by the Potash Company of America near Sussex, New Brunswick. An integrated programme of in situ measurements, laboratory testing and computer modelling was chosen as the best approach to their study and solution.

In situ measurements of deformation and pressure were begun in virgin ground excavations in the ore and in the major evaporite strata surrounding it. These were used primarily for verification of computer models. As our understanding of the response of the rock mass to mining developed, the scope of in situ studies expanded to include active mining areas, which comprise cut-and-fill stopes in potash and open stopes in salt. Backfill in the potash stopes was found to provide a lower support pressure than was anticipated resulting in a destressed zone in the hanging wall in which almost constant strains existed to a depth of at least 15 m.

Strength and creep tests of evaporite core were carried out. The strength and the form of the failure envelopes were typical of salt. Creep test results suggested that a bilinear or curvi-linear relationship existed between shear stress and creep rate; creep rate is increasingly dependent upon stress as stress increases.

Finite element and finite difference computer models were calibrated against the virgin ground in situ measurements and then tested successfully in real design situations. Confidence now exists in their ability to predict stress conditions and deformation rates with sufficient accuracy for routine design.

Resumé

Le gisement de potasse qui est exploité par la Potash Company of America dans la région de Sussex au Nouveau Brunswick pose des problèmes uniques de mécanique des roches à cause de sa forme escarpée et plissée. Un programme complet de mesurage in situ, d'essais en laboratoire et de simulation par ordinateur a été élaboré pour étudier et résoudre ces problèmes.

Les mesures in situ de déformation et de pression ont tout d'abord été effectuées dans des excavations vierges à l'intérieur du gîte minéralisé et dans la strate d'évaporite environnante. Ces données ont servi à vérifier les modèles de simulation. Suite à une meilleure connaissance de la réaction de la masse rocheuse par rapport à l'extraction du minerai, la portée des études s'étendit aux régions d'extraction active comprenant les chambres de coupe et de remblayage dans la potasse et les chantiers ouverts dans le sel. Le remplissage dans les chantiers d'abattage de potasse procure une pression de soutien plus basse qu'anticipé, résultant en une zone de relâchement de tension dans l'éponte supérieure où une tension presque toujours constante existait jusqu'à une profondeur d'au moins 15 m.

Des tests de force et de rampe sur les noyaux d'évaporite furent effectués. La force et la forme des manques de l'enveloppe sont typiques du sel. Les résultats des tests de rampe suggèrent qu'une relation bilinéaire ou curvi-linéaire existe entre la force de cisaillement et la cadence de rampe; la cadence de rampe va en dépendance croissante sur la force, à mesure que la force augmente.

Les modèles informatiques à élément fini et à différence finie ont été calibrés par rapport aux mesures d'excavations vierges in situ et ensuite essayés dans des situations courantes. Il est maintenant acquis que les modèles peuvent être utilisés couramment pour prédire avec une précision suffissante la condition des forces et la cadence de déformation.

Table of Contents

		Page
1	**Introduction**	1
2	**Site Geology and Mine Description**	2
	2.1 Regional Geology	2
	2.2 Stratigraphy	2
	2.3 Structure	4
	2.4 Mine Layout	5
3	**Outline of the Rock Mechanics Programme**	12
	3.1. Alternative Strategies	12
	3.2. Programme Description	13
4	**Underground Instrumentation**	15
	4.1 Description of Instruments	15
	4.1.1 Total Closure Monitoring	15
	4.1.2 Borehole Extensometers	16
	4.1.3 Earth Pressure Cells	17
	4.1.4 Borehole Pressure Cells	17
	4.1.5 Borehole Deformation Gauges	19
	4.2 Measurements of Trial Openings	19
	4.2.1 Upper Halite	19
	4.2.2 Middle Halite	22
	4.2.3 Basal Halite	23
	4.2.4 Potash	24
	4.3 Instrumentation of Stopes	25
	4.3.1 1900-2 Potash Stope	25
	4.3.1.1 Earth Pressure Cells	26
	4.3.1.2 Multi-point Extensometers	27
	4.3.1.3 Closures	28
	4.3.2 Salt stopes	29
	4.3.3 Salt Pillars	29
	4.4 Discussion	30
5	**Laboratory Testing**	33
	5.1 Introduction	33
	5.2 Core Sampling and Sample Descriptions	33
	5.3 Laboratory Facilities	34
	5.4 Test Procedures	35
	5.5 Intact Material Test Results	36

		5.5.1 Brittle Yield Tests	36
		5.5.2 Physical Properties	38
		5.5.3 Creep Tests	38
		5.5.4 Creep Models Proposed	41
	5.6	Backfill Material Model	42
		5.6.1 Literature Review	43
		5.6.2 Proposed Material Model	44
		5.6.3 Computer Implementation	45
	5.7	Laboratory Testing of Pressure Cells	45
	5.8	Discussion	47
6	**Numerical Analysis and Design**		50
	6.1	Introduction	50
	6.2	Computer Codes	51
		6.2.1 GEOROC	51
		6.2.2 FLAC	52
		6.2.3 Boundary Element Programs	53
	6.3	Computer Hardware	53
	6.4	Material Property Validation	54
		6.4.1 Upper Halite	55
		6.4.2 Middle Halite	56
		6.4.3 Basal Halite	58
		6.4.4 Potash	60
	6.5	Large Scale Mine Modelling	63
		6.5.1 Potash Stopes	63
		6.5.2 Salt Stopes	66
	6.6	Discussion	67
7	**Discussion and Conclusions**		70
8	**Acknowledgements**		74
9.	**References**		75

List Of Figures

		Page
Figure 2.1	Location of Potash Company of America lease area	2
Figure 2.2	Stratigraphic column of the evaporite sequence at PCA lease area	3
Figure 2.3	Schematic cross-section of the salt dome	4
Figure 2.4	Typical ore zone cross section at a potash stope	
Figure 2.5	Mine Plan Showing Location of Rock Mechanics Instrumentation	8
Figure 2.6	Typical ramp and stope layout for lower level potash stopes	6
Figure 4.1	Borehole rod extensometer with snap ring anchor	16
Figure 4.2	Earth pressure cell installation	18
Figure 4.3	Cylindrical borehole pressure cell	18
Figure 4.4	CANMET borehole deformation gauge	19
Figure 4.5	Instrumentation layout in rock mechanics room (178+00 cross cut)	20
Figure 4.6	Total horizontal closures in the rock mechanics room	20
Figure 4.7	Pressure cell readings in the floor of the rock mechanics room	21
Figure 4.8	Pressure cell readings in the west wall of the rock mechanics room	21
Figure 4.9	Extensometer measurements from the Upper Halite, 189+00 cross cut	22
Figure 4.10	Closure rates of cross cuts in the Middle Halite	23
Figure 4.11	Extensometer measurements in the 1500-2 east tailings cross cut (station 33)	23
Figure 4.12	Location plan of stations 51 and 52 in the Basal Halite, 1900 level main entry	23
Figure 4.13	Closure rates at various points along 1906 main entry	23
Figure 4.14	Total closures in the Basal Halite at stations 51 and 52	24
Figure 4.15	Extensometer readings from north wall at stations 52, Basal Halite	24
Figure 4.16	Instrumentation layout in the 189+00 cross cut	25
Figure 4.17	Total closures measured in potash and salt in 189+00 cross cut	25
Figure 4.18	Extensometer readings in Potash in the 189+00 cross cut	26
Figure 4.19	Instrumentation layout at 140+00 section of 1900-2 stope	26
Figure 4.20	Earth pressure cell readings from lift 4 of 1900-2 stope	27
Figure 4.21	Extensometer readings from the footwall of 1900-2 stope, 4th lift	28
Figure 4.22	Extensometer readings from the hanging wall of 1900-2 stope, 5th lift	28
Figure 4.23	Closure rates on successive lifts in the back of the 1900-2 stope (legend numbers indicate mine sections)	28
Figure 4.24	Instrumentation layout at main entry cross cut intersection at 172+50	29
Figure 4.25	Expansion in the south wall of salt pillar	30

Figure 4.26	Expansion in the west wall of salt pillar	30
Figure 5.1	Failure stress states in brittle yield tests	36
Figure 5.2	Potash sample P11	39
Figure 5.3	Potash sample P18	39
Figure 5.4	Potash sample P216A	39
Figure 5.5	Potash sample UH40A	39
Figure 5.6	Upper Halite sample UH2730B	40
Figure 5.7	Basal Halite sample LH1516	40
Figure 5.8	Mean stress effects on the creep rate of Potash	40
Figure 5.9	Particle size distribution for mine tailings	43
Figure 5.10	Moisture content in a vertical section of fill 6-12 months old	43
Figure 5.11	Comparison between proposed model and experimental data	44
Figure 5.12	Comparison between closure of filled and unfilled salt stopes	44
Figure 5.13	Pressure cell test apparatus	46
Figure 5.14	Pressure-time response of resin encased cell	47
Figure 5.15	Pressure-time response of potash encase cell	47
Figure 6.1	Finite element mesh for single drift calibration models	55
Figure 6.2	Predicted inelastic closures in the Rock Mechanics Room	55
Figure 6.3	Predicted wall expansion in Upper Halite in the 189+00 cross cut	56
Figure 6.4	Predicted steady state pressure distribution in the wall of the Rock Mechanics Room	56
Figure 6.5	Total closures predicted by the power bilinear laws compared to field measurements	57
Figure 6.6	Predicted wall deformation using bilinear power law	57
Figure 6.7	Finite element mesh used for main entry drift simulations	58
Figure 6.8	Total measured closures compared to closure and wall expansion predictions using the power law	59
Figure 6.9	Measured closures compared to total closures and wall expansion predicted by the bilinear law	60
Figure 6.10	Finite element mesh used for simulation of 189+00 cross cut	61
Figure 6.11	Comparison of predicted and measured closures in potash in the 189+00 cross cut	61
Figure 6.12	Comparison of measured and predicted wall expansion in 189+00 cross cut	62
Figure 6.13	Finite element mesh used for 1900-2 stope simulation	64
Figure 6.14	Detail of the FLAC mesh used for 1900-2 stope simulation	64
Figure 6.15	Principal stress vectors from FLAC simulation	64
Figure 6.16	Footwall expansions predicted by GEOROC simulation	65
Figure 6.17	Hanging wall extensions predicted by GEOROC simulation	65
Figure 6.18	Horizontal closure velocities around salt stope 30	66

List of Tables

Table 5.1	Elastic constants and strength envelope parameters for PCA evaporites	37
Table 5.2	Physical properties of PCA evaporites	38
Table 5.3	Creep law constants for PCA evaporites	42

1. Introduction

Potash Mining in New Brunswick presents challenges which differ significantly from those of mining other deposits in North America. The ore varies widely in thickness and may be lying at almost any angle, perhaps changing from horizontal to vertical within a few tens of metres. At the Potash Company of America mine near Sussex, N.B. this dictates that mining must take place on many different levels using a continuous "cut and fill" method not often used in other potash mines. The result is a unique set of problems in designing the layout and sizes of stopes and access drifts.

The potash industry has traditionally relied upon experience and instrumented full scale trials to develop mine layouts which minimize ground control problems. This process can be called an observational approach to design and is exemplified by Baar (1977). However, when faced with unique conditions, prior experience is only of limited value; critical design decisions may have to be made before adequate observational information has been amassed. With these problems in mind, a decision was made in 1986 to implement a structured rock mechanics programme at the mine.

Stated broadly, the purpose of the programme was to develop an understanding of the way in which the rock mass responds to mining and to use this understanding to help provide a stable environment in which ore extraction can be maximized and the safety of underground workers is ensured. In order to achieve this within a reasonable length of time it was necessary to integrate in situ monitoring, laboratory testing and numerical modelling to form the basis of a design and assessment system. Through initial use as an aid to interpretation of in situ measurements, confidence in modelling is expected to grow until it becomes the dominant design method.

Recognizing that the proposed rock mechanics study involved a substantial research component, the results of which could be of benefit to the mining industry, the New Brunswick Department of Natural Resources and Energy agreed to participate in its funding. Funds were provided under the Canada - New Brunswick Mineral Development Agreement. The programme was established in 1987 and work began in August of that year.

Despite the research components of the programme, its success must ultimately be judged by the way in which it has altered the perception and practice of rock mechanics at the mine, not upon its academic merits. It should lay a foundation upon which sound rock mechanics design and monitoring can be based for the lifetime of the mine. This viewpoint is reflected throughout the programme and in some cases resulted in the use of techniques or methods which are not the 'state of the art' but are more reliable or more easily applied. The remainder of this report describes specific details of the programme and recommends ways in which the progress made can be built upon in the future.

2. Geology and Mine Layout

2.1 Regional Geology

PCA mines potash and salt from a northeasterly trending anticline, or salt pillow, in the Sussex-Petitcodiac area of southeastern New Brunswick. (Figure 2.1) This anticline is at least 27 km in length, up to 1000 m thick and comes to within 100 m of surface, where it displays early stages of diapirism.

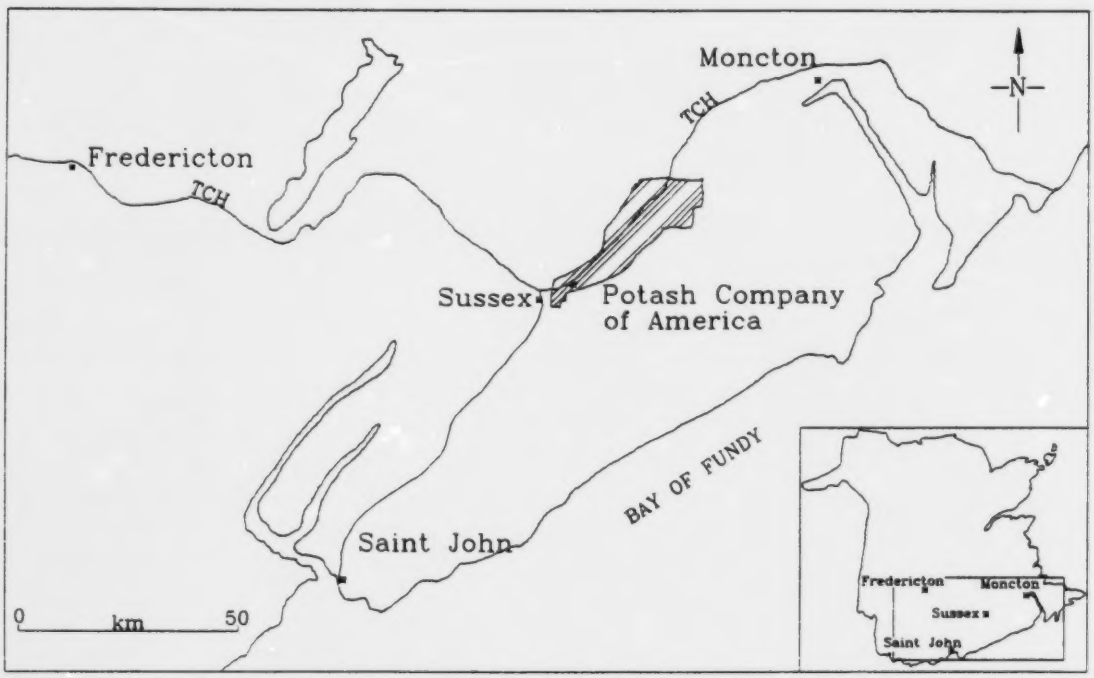

Figure 2.1 Location of Potash Company of America lease area

Potash was initially discovered in 1973, in a drilling programme initiated by the New Brunswick Department of Natural Resources. Later work by PCA determined the stratigraphy and structure of the deposit as well as establishing an ore grade and tonnage. Mining, which began in 1983 is currently producing 2,000,000 tons potash ore (sylvinite) and 500,000 tons rock salt per year.

2.2 Stratigraphy

The evaporites (Windsor Group) were formed as a result of two marine incursions in what is otherwise a clastic red bed sequence. The first marine cycle deposited a thick sequence

of carbonates and sulphates (the Upham Formation) overlain by higher order evaporites (the Cassidy Lake Formation) including the potash ore bed. The second cycle (Plumweseep Formation), which is a similar but less well developed sequence, and does not include potash mineralization, is capped by a grey claystone. (Figure 2.2)

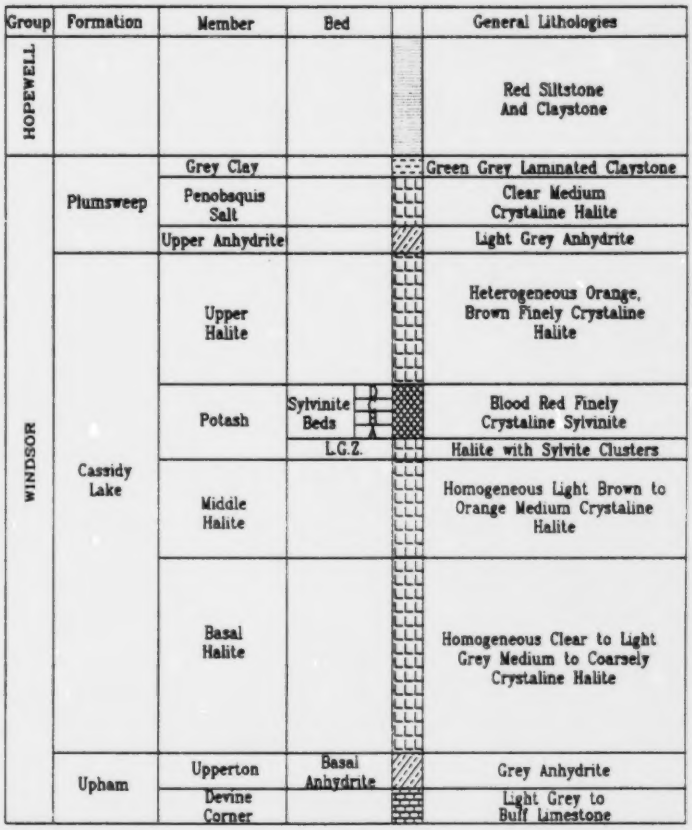

Figure 2.2 Stratigraphic column of the evaporite sequence at PCA lease area

The lower most unit of the Cassidy Lake Formation - the Basal Halite Member - is composed of clean clear halite with minor zones of anhydrite laminae. This is overlain by the argillaceous Middle Halite Member which contains weakly bedded scattered inclusions of grey green to red brown clay making up approximately 5% of the total lithology. The contact with the overlying Potash Member is gradational. This member is made up of a Lower Gradational Zone, overlain by sylvinite beds which can be subdivided into A, B and C Zones and a D Zone of interbedded sylvinite and halite. The hanging wall salt, or Upper Halite, close to the ore, is largely fine to medium grained clear halite with zones of weakly bedded argillaceous halite. Higher in the section, towards the top of this evaporite cycle, the lithology becomes more heterogeneous with many thin argillaceous beds present.

The second evaporite cycle is preserved on the lower flanks of the present salt structure. On the crest of the anticline, the salt has been suberoded and the Upper Anhydrite is intermixed with the overlying grey claystones. Suberosion has also lead to the development of a residual bed representing the preserved insoluble fraction of the various members of the Cassidy Lake Formation.

Friable, jointed, waterbearing claystones of the Hopewell Group are the dominant lithology overlying the evaporites.

2.3 Structure

As indicated earlier, the evaporites form a northeasterly trending anticlinal feature, plunging at 5° to the northeast. While the flanks of the anticline have a nominal 45° dip, large scale, open, recumbent folding is also present (Figure 2.3). Within the evaporite sequence, halokenesis has led to folding on various scales. The Basal Halite is highly foliated and extensively recrystallized, with tight isoclinal folding present near the axial plane of the main anticline, while on the limbs, open drag folds with a wavelength of a few tens of metres, are common. This style of folding extends into the Middle Halite and Potash Members. However, in the ore zone, evidence of differential flowage is ubiquitous, particularly near the upper and lower contacts, where dislocation and boundinaging of halite beds are common.

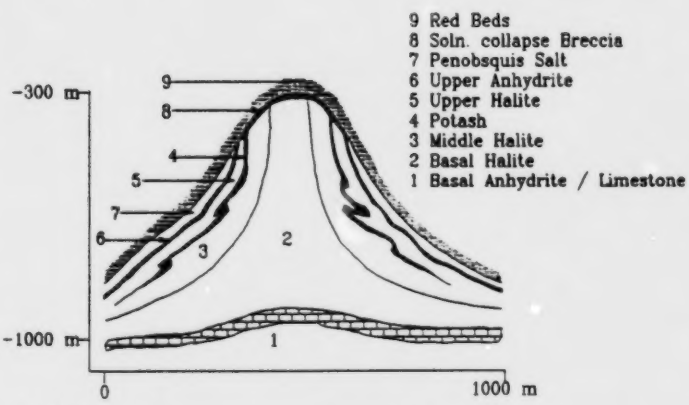

Figure 2.3 Schematic cross-section of the salt dome

Typically, the A Zone of the Potash Member is quite regular with small scale drag folds having an amplitude of 25 cm and a wavelength of less than 1 m, while the upper part of the C Zone and the D Zone are characteristically more chaotic with irregular drag folding on a much larger scale. The degree of deformation decreases in the Upper Halite although large scale open drag folding is typically present. A typical ore zone section, as seen at a mining face, is shown in Figure 2.4.

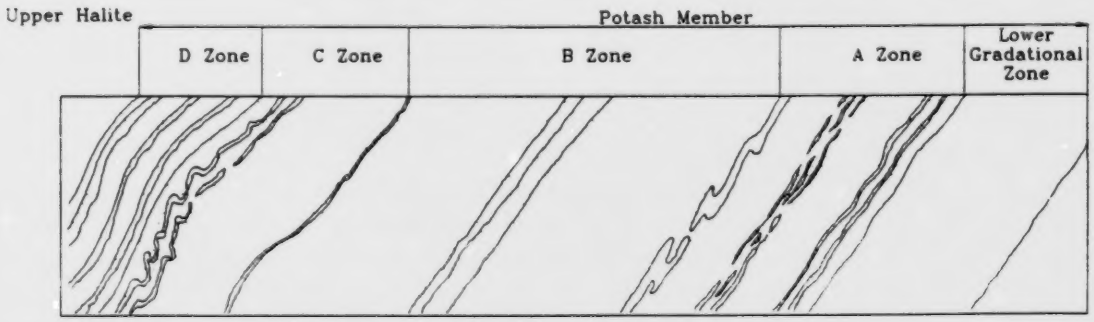

Figure 2.4 Typical ore zone cross section at a potash stope face

In the Potash Member, it is common to find extensive areas where the potash mineralization has been completely leached out. These barren zones of discoloured halite - known as Salt Horses - generally occur in the A Zone and upper C Zone to D Zone and, although aerially extensive, are usually thin. However, they sometimes affect the complete ore zone, in which case more extensive deformation is typical together with an associated irregular halo of very coarse grained recrystallized euhedral clean sylvite and halite.

Occasional slickensides have been identified in the Potash Member with indications of movement parallel to dip. The relationship of these features to the other structures identified in this Member is not known at this time.

2.4 Mine Layout

Access to the mine is through two 5 m diameter shafts sunk on the north flank of the anticline. These shafts are concrete lined to the contact with the top of salt at around 470 m and screened below this elevation to the main development level (1900 level) at 580 m. Overlapping 300 m radius pillars are left around each shaft, within which no production takes place. However, the underground mine shop complex together with salt and potash storage bins, salt crusher and screening area, is developed within the shaft area. Most of this development is in the order of 3 m high by 8 m wide.

Potash and salt stopes extend eastwards from the shafts and are accessed from twin parallel drifts, developed in the Basal Halite, running close to the contact with the Middle Halite. Exploration is carried out from a drift in the ore zone at approximately the same elevation as the access drifts. A composite mine plan, indicating the major mining elements and the locations of all rock mechanics instrumentation referred to later, is provided in Figure 2.5

Potash stopes are developed both above and below the main level, connected by cross cuts through the Middle Halite to the access drifts. A typical stope (Figure 2.6) is in the order of 800 m long with a vertical height of 120 m. This block of ore is defined by tailings ramps at either end, connected by a basal sill cut, and split by a central ramp used to convey ore from the stope.

Salt tailings from the milling process is conveyed into the side of the stope which has just been mined through, then spread out and compacted by scooptrams to within 2.4 m from the back. While this fill is being placed in one half of the stope, the continuous mining machine is taking another cut in the other half of the stope. The mining machine, which is tracked, rides on recently placed fill and cuts a 4.3 m high brow from hanging wall to footwall. The width mined varies according to the width of the ore and can range from less than 10 m to as much as 40 m. The profile of the cut is dictated by the dip of the

ore zone contacts, although structural irregularities in the hanging wall together with the need to mine the D Zone for ground control purposes in areas of low dip, lead to deviation from the plan in certain areas. Broken ore is picked up by the mining machine, as it advances, and conveyed out of the stope, up the ore ramp and along the cross cut to the mainline ore conveyor in the main access drift.

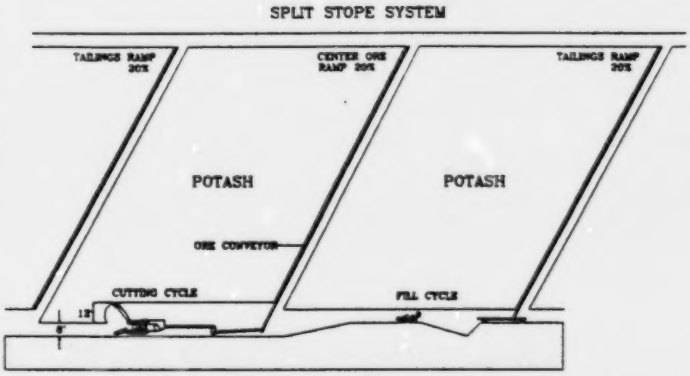

Figure 2.6 Typical ramp and stope layout for lower level potash stopes

Ore is mined from stopes above the main level in a manner similar to that used in the lower stopes. Using the exploration drift on the main level as the sill cut the stope is mined progressively higher while ramps are constructed on fill at either end.

This mechanized cut and fill method of potash mining allows extraction of an extremely high percentage of the ore. Only a single 12 m crown pillar is left between the upper and lower series of stopes while individual stopes within the series are mined without the need for intervening pillars. Pillars are also left around surface exploration drill holes, although these were routinely grouted from their total depth to surface. These are a minimum of 30 m in radius, similar to the distance that will be left from the upper most mine working to the Upper Anhydrite or the caprock.

South of the two main access drifts, stopes are developed in the Basal Halite; typically they are in pairs to allow flow-through ventilation. The actual layout of these stope pairs is dictated by the distance to the contact with the Middle Halite on the south flank of the anticline. As they were initially mined for tailings and slimes storage during early development of the potash stopes, and later as storage for mill brine in excess of plant evaporator capacity, they are developed below the main access level. A completed stope is in the order of 300 m long, 23 m wide and 18 m high, with pillar widths of some 20 to 60 m. These stopes are mined using the same roadheader machines as are employed in the potash stopes, by taking progressively lower cuts in the floor to give the final dimensions noted above. As in the potash stopes, no artificial ground control is required.

Future development will progress towards the east as an extension of the present mine layout. However, this will be modified as required by the geology of the ore body. Further east, the ore extends over a greater dip length than in the area presently being mined. This will lead to the need to establish both a shallower and a deeper series of stopes. The ore also becomes wider further east, such that modifications to the high

extraction mining techniques presently employed may be required. Also areas of large scale isoclinal folding, where present further east, may lead to the development of multilevel mining.

Given the present mining rate and planned development, none of these modifications to the present cut and fill mining need be considered until some time in the future.

The development of salt stopes to the east has kept pace with potash stope development. However, given the increasing distance from the shaft both for conveying mined salt and the return of brine and slimes, a future series of deeper salt stopes will be developed. This will decrease transportation distances and allow mining of some of the high quality salt which exists beneath the present 1900 level.

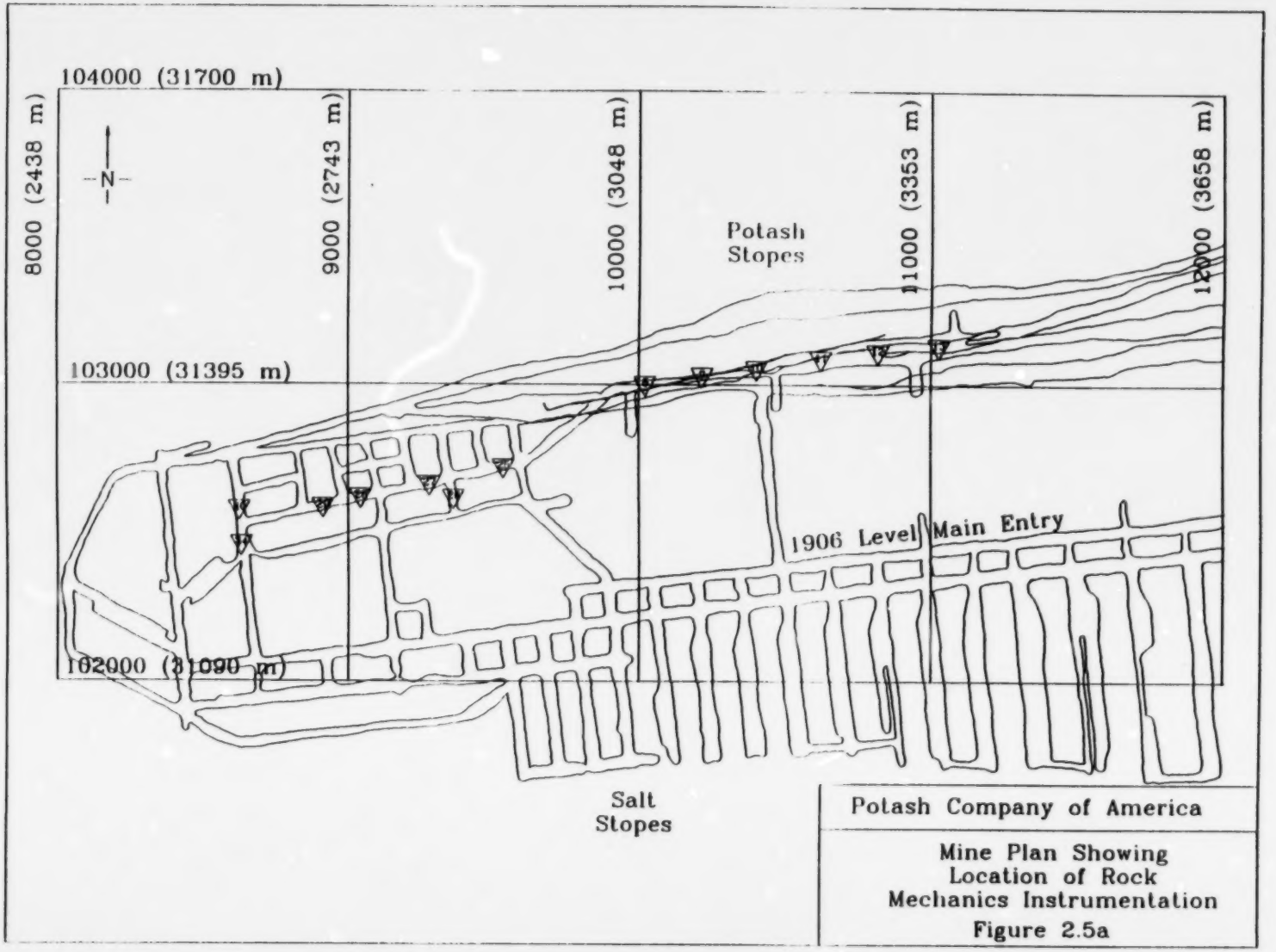

Potash Company of America

Mine Plan Showing
Location of Rock
Mechanics Instrumentation

Figure 2.5a

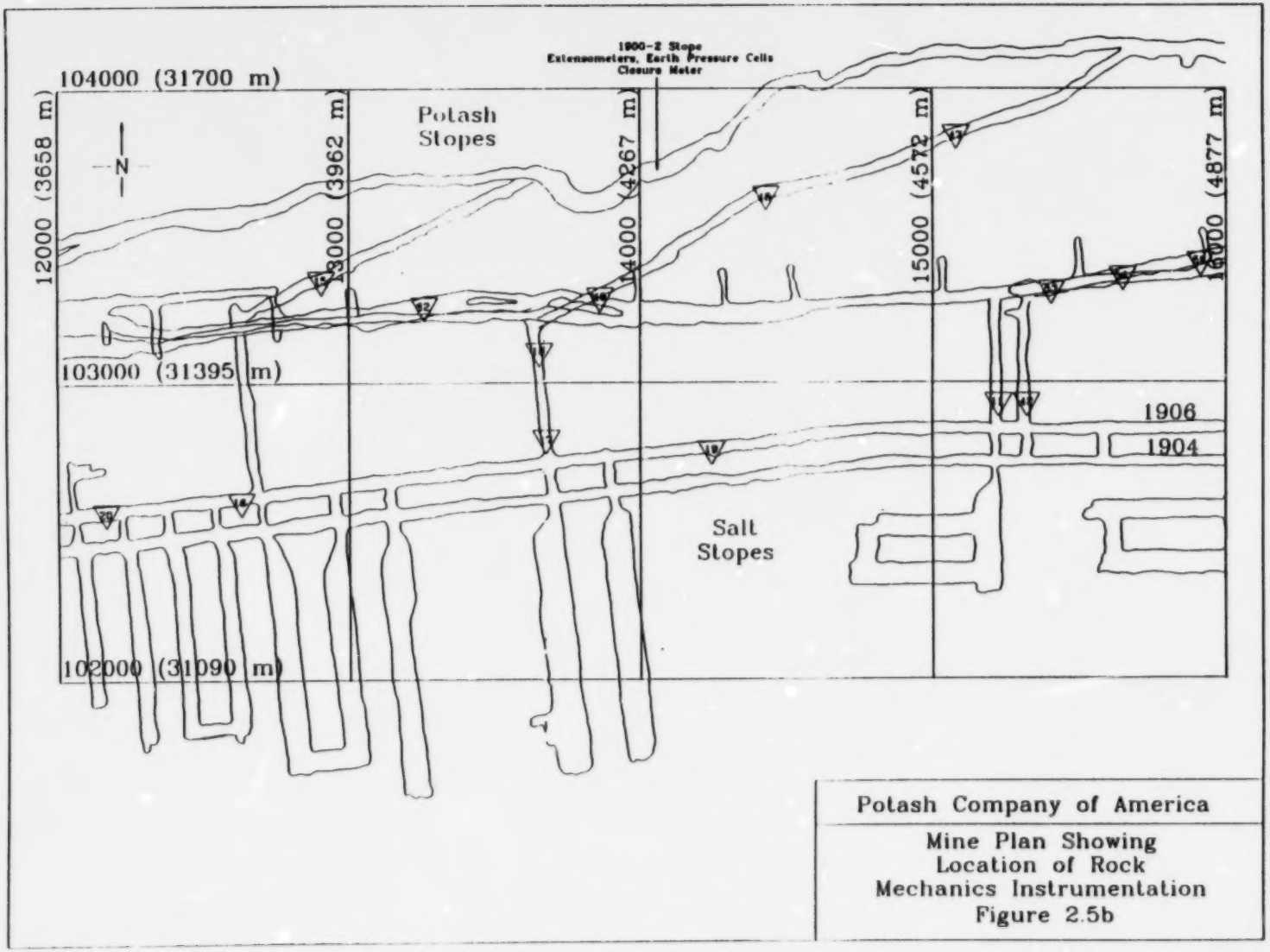

Potash Company of America

Mine Plan Showing
Location of Rock
Mechanics Instrumentation
Figure 2.5b

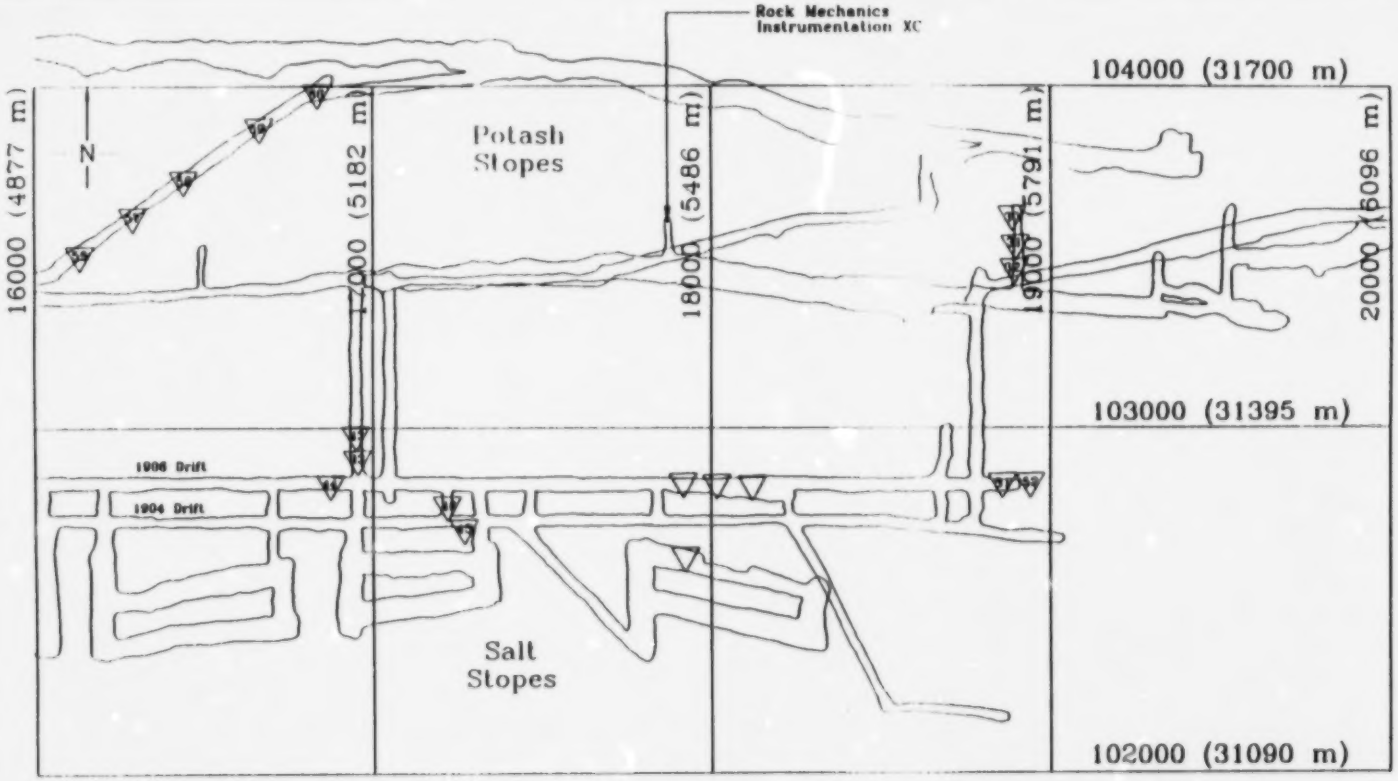

Potash Company of America

Mine Plan Showing Location of Rock Mechanics Instrumentation

Figure 2.5c

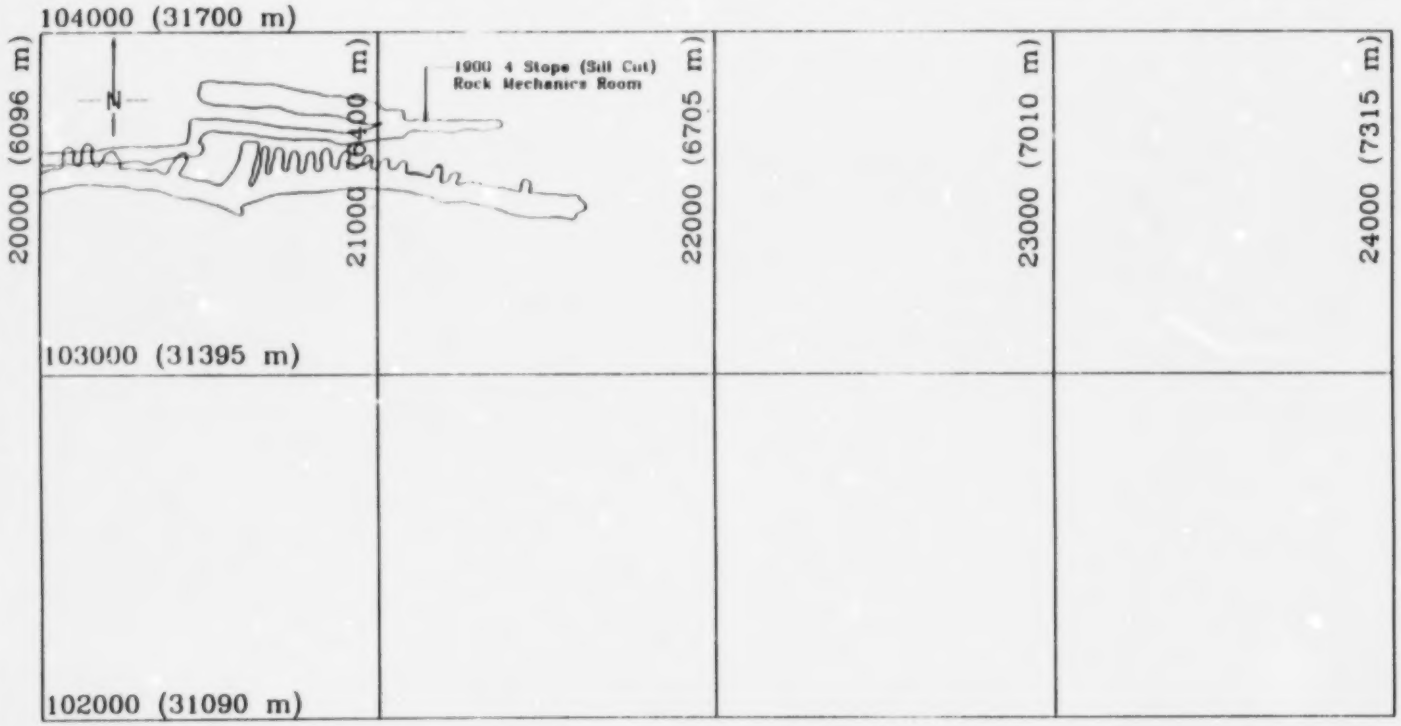

Potash Company of America

Mine Plan Showing
Location of Rock
Mechanics Instrumentation
Figure 2.5d

3. Outline of the Rock Mechanics Programme

The aim of the rock mechanics programme was to develop rational methods for design which would ensure a safe and economic approach to mine planning. While it was recognized that this goal would not necessarily be achieved within the two year duration of the programme, it was essential that a framework be established which would permit the assimilation of information gathered in the future. Most importantly, the programme had to demonstrate the value of rock mechanics to mining practice by developing a basic design capability and methods of measurement by which design assumptions can be verified.

3.1 Alternative strategies

Alternative strategies for developing and implementing rock mechanics design methods were considered at the outset. Three are commonly used. The first is to adopt an entirely observational approach, essentially similar to that used in the early years of Saskatchewan potash mining. Given sufficient observations of rock mass response under a wide variety of geological and geometrical conditions it is possible to develop guidelines for the most effective dimensions for different mining elements. The drawbacks of this approach are that it takes a great deal of both time and data. One mine can only generate enough data in a reasonable time if the geology is extremely consistent. Such is the case in Saskatchewan but New Brunswick presents a much more complex problem. Also, while design methods derived in this way may be effective, they will not necessarily be efficient unless both stable and unstable excavations can be studied because that is the only way factors of safety can be evaluated.

The second approach is to rely entirely upon prior experience. Other mines which have operated for a long period under similar conditions are a source of information which can be used for design. An example is the coal mining industry where exhaustive analysis of many case histories has given rise to a wealth of empirical design procedures which are very effective when applied under the right conditions. Unfortunately, the evaporite mining industry has not had the coherence to develop such guidelines and there is no one mine at which conditions are sufficiently similar to those at PCA to be of direct value. Prior experience can also be used in numerical modelling. If suitable computer programs or analytical methods exist and the literature contains the necessary material constants, acceptable designs may be based upon them. Unfortunately, for visco-plastic rocks, the material constants vary quite widely and computer programs with the required capabilities are all, to varying extents, experimental.

The third approach is one in which observation and numerical modelling are integrated to produce a design procedure in which modelling is guided and verified by in situ measurements. This approach offers the benefits of being relatively quick to implement

and being applicable to more general predictions than the observational approach. It was this strategy which was adopted for the Rock Mechanics Programme.

3.2 Programme Description

In the integrated approach the requirements for field observations are rather different than in a purely observational approach. Rather than instrument the active mining areas, it is necessary to develop and monitor excavations designed specifically for the purpose of verifying numerical models. The first task in the programme was thus to choose or mine virgin ground excavations in each of the main stratigraphic units. These were chosen on the basis of simple geometry (usually rectangular) and straightforward geology. Ramps, exploration drifts and diamond drill stations provided ideal sites and only two excavations were specially created. Instrumentation used in these locations was simple and easily installed so wide coverage could be obtained. Extensometers and total closure points were used extensively and were augmented in some areas by pressure cells.

Core samples of the evaporites were obtained by diamond drilling from the virgin ground excavations. They were sent to the University of Waterloo for laboratory testing. Elastic and visco-elastic properties were determined in a series of triaxial tests. These parameters were then used in numerical models of the excavations as first approximations of the mechanical properties of the rock mass.

The establishment of a numerical modelling capability required choosing a complete system of hardware and software. A decision was made to purchase Compaq Deskpro 386 computers (IBM compatible) although at that time they would not support any suitable rock mechanics software. Some difficulties were originally encountered finding suitable operating systems and language compilers but the range of 80386 expanded dramatically in early 1988 and the problems were quickly overcome. The Phar Lap Tools extensions to MS-DOS were purchased which allowed unrestricted access to extended memory, permitting the transfer of any mainframe or minicomputer programs to the Compaq. A selection of rock mechanics programs and other engineering and graphics programs were then obtained which satisfied all the computing requirements of the rock mechanics group.

Using a finite element program, models of the test excavations were created. The results given by these models were compared to the actual behaviour of the test excavation and the adjustments were made to the parameters of the material constitutive law until an acceptable fit was achieved. Once this process had been completed for all the test excavations, models of more complicated excavations were prepared. Predictions of in situ behaviour were made from these models and instrumentation was installed in the mine to verify the accuracy of the predictions. Extensive instrumentation of the 1900-2 potash stope was carried out for this reason.

Once modelling had been developed to this extent, its use for design and mine planning

was begun. Simple designs for salt stopes and barrier pillars have been performed and mining is being monitored to verify the designs. Eventually it is hoped that empirical design guidelines can be derived from the results of numerical models and will replace them for routine design.

4. Underground Instrumentation

Instrumentation has a variety of uses in rock mechanics. It can be used to help in the development of hypotheses, to demonstrate the validity of those hypotheses and lastly to provide a warning if an excavation is not behaving according to that hypothesis. The first two uses are of main significance in the rock mechanics programme; the goal is to reach a stage at which the rock mass behaviour is sufficiently well understood that only the final use will be necessary.

At the outset of the programme, small excavations remote from high extraction mining areas were instrumented to collect rock mass property information specific to the four evaporite beds. Later, instrumentation was placed in the active mining areas to confirm that on a large sale, the rock mass behaved in a way which could be predicted by modelling. Concurrently, many areas of the mine were instrumented as part of a long term monitoring programme intended to provide indications of local or widespread instability. Each of these sets of instrumentation and the results they produced will be discussed in detail in the following sections.

4.1 Description of Instruments.

The range of instruments chosen for use in the programme is described below. The choice of instruments was dictated by robustness and ease of use. Sophisticated remote data acquisition systems were avoided because of the harsh environment (wet, salty air and dust) in which they would have to operate and the very long cable runs needed to centralize the system sufficiently to make it worthwhile. Further, it was felt that unless a central data acquisition system is necessary for safety reasons, its impact is negative to the extent that it discourages direct observation of conditions in the instrumented area.

4.1.1 Total Closure Monitoring

a) Tape Extensometer.

Widespread use of total closure points was made. Total closures are a convenient way of monitoring changes in the loading conditions around an excavation due to both mining activity and load redistribution resulting from creep. Measuring points consisted of eye screws with 20 mm eyes and 30 mm long, 6 mm diameter self-tapping screws. Holes were drilled in the evaporite with a cordless hand drill and multi-purpose bit. The eye screws were then screwed in with pliers.

The distance between eye screws was measured with a Geokon model 1600 tape extensometer. This unit employs a steel tape under constant spring tension and distances

are read to a resolution of +/- .001 in. by means of a dial gauge.

b) COR-P Closure Gauge

Remote measurement of closure within backfilled stopes was carried out with the Roctest COR-P instrument. It is a telescoping prop which is anchored to the stope walls at either end, with deformation measured by means of a rotary potentiometer mounted inside the telescoping tubes. The instrument has a range of approximately 900 mm and is 1.8 m long. 100 mm diameter well casing was used to extend the length of the instrument to match the width of the stope. As protection against vertical pressure from the fill it was mounted inside a 400 mm diameter flange-nested culvert.

4.1.2 Borehole extensometers

Mechanical extensometers with a length of 9 m or less were manufactured locally to our own design. The anchors were fabricated from 50 mm aluminum bar and held in place by two snap rings. 13 mm threaded rod screwed into the anchors and extended to the collar of the borehole where there was a stainless steel reference plate and guide tube. The depth to the end of the threaded rod from the face of the reference plate was

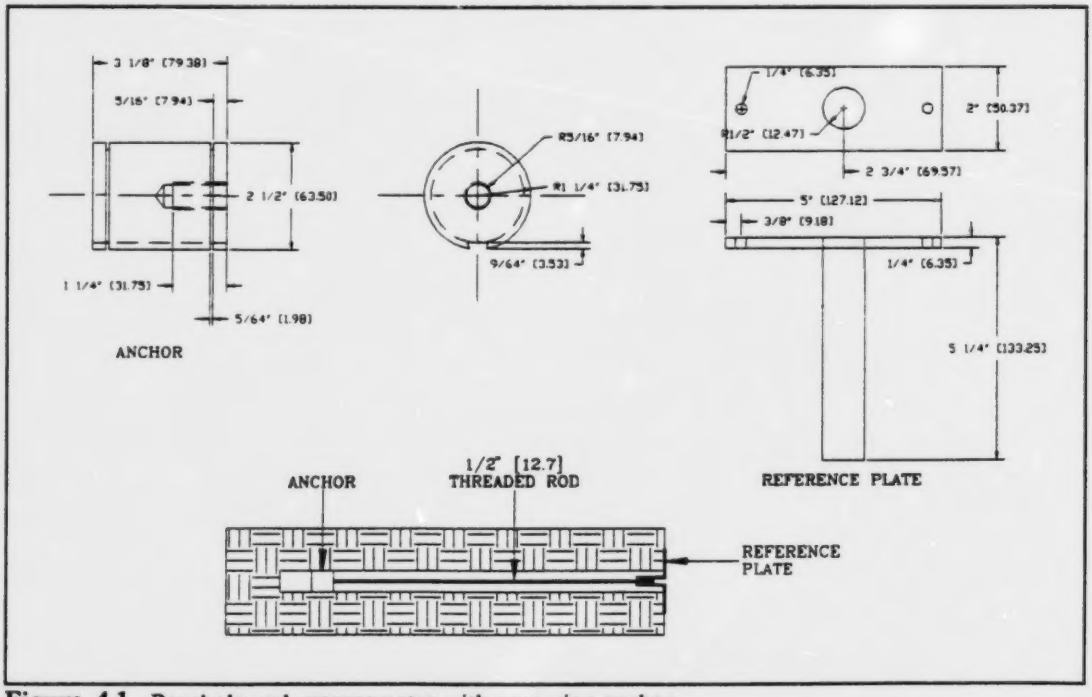

Figure 4.1 Borehole rod extensometer with snap ring anchor

measured with a dial gauge to an accuracy of ±.025 mm (.001 in.). The complete system is shown in Fig. 4.1. The advantages of this extensometer were low cost, easy installation and reading, and good durability. Extensometers in which the head protruded from the borehole usually had a very short lifespan. Scoop trams and other mobile equipment invariably hit any exposed instruments so a flush or recessed mounting greatly improves durability.

Longer extensometers and those requiring remote data acquisition were obtained from commercial sources. The unit chosen was the Roctest WR-FLEX preassembled multi-point extensometer which is available with an electronic head attachment. The extensometer can be ordered with 5 anchors set at any combination of depths and is grouted into a hole of 40 mm or greater diameter. The electronic head operates by threaded extensometer rods driving precision rotary potentiometers having a range of 150 mm and a resolution of +/- .01 mm. A Type 50 Portland cement and water grout with a water/cement ratio of 0.6 was used for most installations. Grout was poured into down holes before inserting the extensometer. In up holes it was pumped through a grout tube at the collar of the hole, using a hand pump, until grout emerged from a vent tube taped to the deepest anchor of the extensometer.

Some reliability problems were experienced with the electronic system but it was generally felt that the WR-FLEX represented a reasonable combination of ease of use and economy.

4.1.3 Earth Pressure Cells

Pressures in the backfill of an active potash stope were measured using hydraulic/electronic pressure cells. Geokon model 4800E cells with a maximum pressure of 7 Mpa (1000 psi) were chosen. These were 180 mm diameter stainless steel hydraulic wafer cell with a built-in pressure transducer. Cables were run to ramps where manual reading with Geokon GK-401 vibrating wire readout could be performed.

The earth pressure cells were sealed into plastic bags for protection from brine then packed in a bed of 200 mm to 300 mm of clean silica sand to ensure even pressure distribution. Tailings was then packed around them by hand before scoop trams were allowed to backfill over them. The installation is illustrated in Figure 4.2.

The earth pressure cells proved to be very reliable. In retrospect, the cells could have had a lower maximum rated pressure with correspondingly improved resolution. However, the resolution of +/- 1.7 kPa provided by these cells was adequate.

4.1.4 Borehole pressure cells

In evaporites it is common to assume that a soft inclusion pressure cell will reach

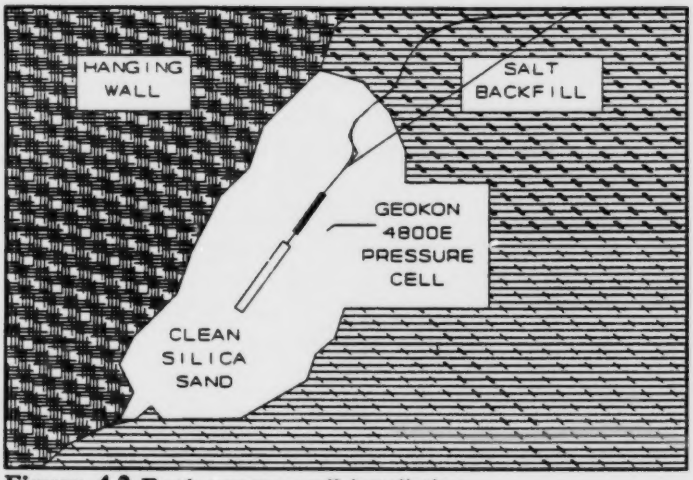

Figure 4.2 Earth pressure cell installation

equilibrium with the rock surrounding the borehole at a pressure equal to the mean in situ stress. Creep of the rock mass surrounding the cell is expected to be sufficient to bring about such an equilibrium. The Saskatchewan Research Council encapsulated flat jack pressure cells used at the beginning of this programme rely upon this assumption for their operation. The cells comprise thin-walled copper wafers filled with hydraulic oil which are connected to pressure gauges by small diameter stainless steel tubing. The wafers are encased in an epoxy resin tube which should fit the borehole to a close tolerance. Once inserted in the hole and oriented in the desired direction, a proof load is applied with a hydraulic hand pump before the system is isolated by closing a valve. The cell reaches an equilibrium with the in situ stress over a few days or weeks and thereafter responds immediately to changes in stress. The thin wafer is assumed to respond only to stresses applied perpendicular to its plane face and is thus capable of measuring stress in a single direction.

The cells described above are widely used in Saskatchewan and have been found to work well in certain situations. Their accuracy under hydrostatic, load controlled conditions has been verified by Denison Potacan (1987). It appears that in the very highly stressed and rapidly creeping ground which surrounds most excavations in Saskatchewan mines, the short comings of the design are usually not noticed or are unimportant. However in the conditions under which they were being used in this programme it was found that the creep of the epoxy casing was sufficient to affect the equilibrium pressure of the cell. Thus, although the indicated pressures were significant in a relative sense, they did not quantitatively represent the in situ stresses.

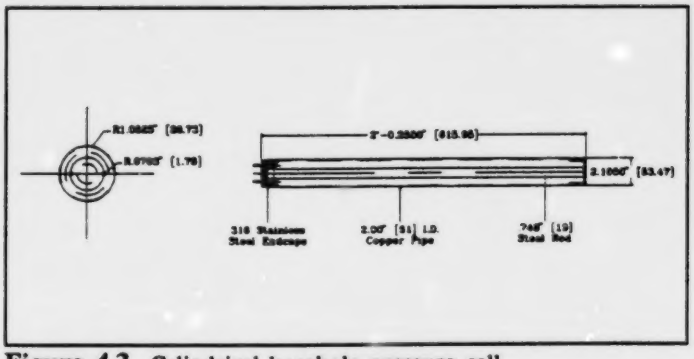

Figure 4.3 Cylindrical borehole pressure cell

Other encasing materials and a different cell design were tested in a small laboratory and

field programme. It was found that cement grout provided a much more stable cell encasement than either epoxy or potash and that its low creep rate in comparison to the evaporites was required to offset the lack of end restraint on the pressure cell in a borehole. A cylindrical copper cell was also tested, with limited success. It is illustrated in Figure 4.3. Fabrication quality was the principal problem encountered with the cylindrical cell; in other respects it was a useful instrument. The results of this testing programme are reported in more detail in Chapter 5.

4.1.5 Borehole Deformation Gauges

Continuous logging of the diameter of boreholes was performed with a vibrating wire strain gauge instrument designed and manufactured by CANMET. The unit was wedged into a 75 mm diameter borehole and connected to a plucking circuit and a continuous data logger. Changes in the borehole diameter were measured to a sensitivity of +/-.0025 mm which was sufficient to establish a closure rate within a few days. The instrument was used to compare strain rates on different axes of a hole, as an indirect method of determining earth pressure ratios, and to locate stress concentrations within pillars. The system has considerable application in potash mining and its use at PCA is likely to become more frequent in the future as its capabilities become fully appreciated. The system is shown schematically in Fig. 4.4.

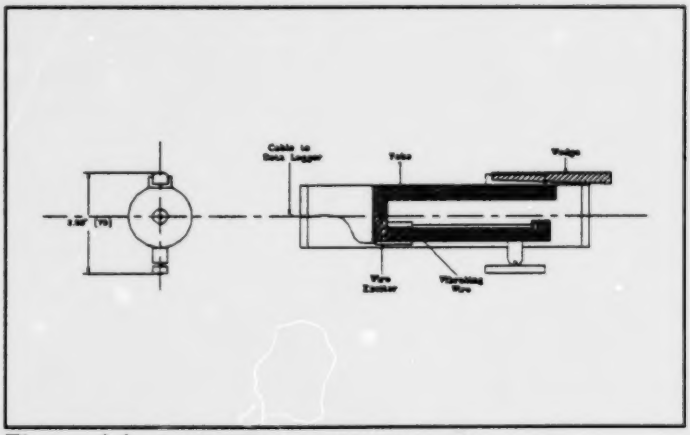

Figure 4.4 CANMET borehole deformation gauge

4.2 Measurements of Trial Openings

4.2.1 Upper halite

The first opening created for taking rock mechanics readings was a 6 m x 3 m cross-cut to the north of the 1850 exploration level at a depth of 550 m below surface. It was cut on August 4 to 7, 1987 at section 178+00 and closure points were installed behind the miner as it cut the opening. Borehole pressure cells were installed by August 15 and rod

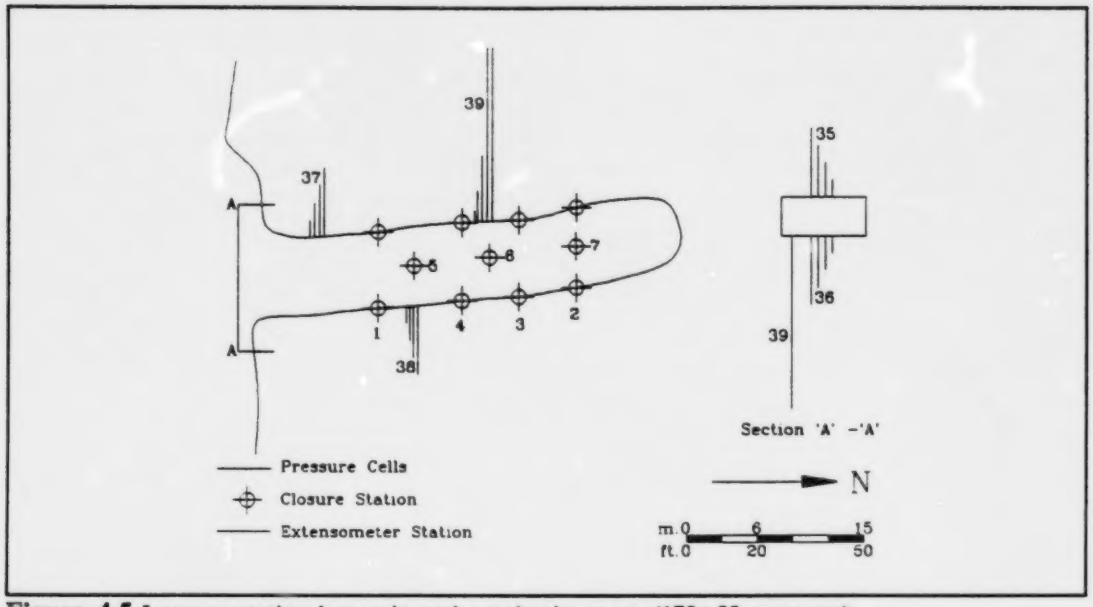

Figure 4.5 Instrumentation layout in rock mechanics room (178+00 cross cut)

extensometers were added several months later, once the tractor mounted drill was available. The instrumentation layout is shown in Figure 4.5.

The behaviour of the drift was initially characterized by exponentially decelerating closure. Fig. 4.6 shows the vertical and horizontal closure at points in the drift referred to in Fig 4.5. Closure rates decay to a rate of less than .002 mm per day and reach an approximately steady state. Extensometers reveal that the immediate roof of the drift is separating slightly and that all horizontal closures are accounted for by deformations in the first 6 m of the rib. Movements in the extensometers are of the same order as the resolution of the instruments, thus it is only possible to consider the major trends in the data.

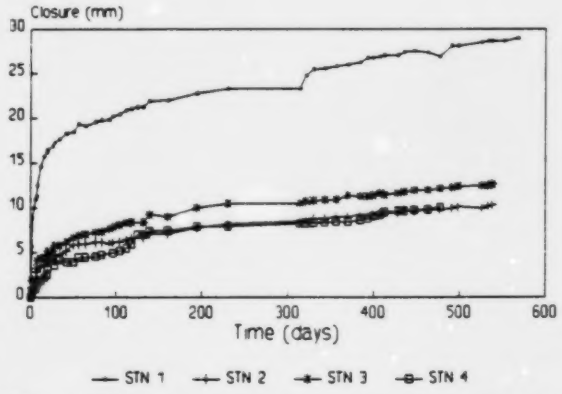

Figure 4.6 Total horizontal closures in the rock mechanics room

The very low creep rates are responsible for erroneously low readings in the copper wafer pressure cells. The cells were installed in 54 mm boreholes and orientated to read either vertical or horizontal pressures. The assumption was made that these orientations were two of the three principal stress directions. Once in place, the cells were pressured to

7 MPa or 17.24 MPa (cells placed to depths of 1.2 m to 1.5 m were pressurized to the lower pressure). The pressure circuits were isolated from the pump once the proof load was applied. Relaxation of the salt surrounding the borehole then resulted in a partial loss of pressure before a slight recovery. Finite element analyses indicated that creep of the salt was such that up to two years would be taken before equilibrium between the cell and the borehole wall was reached. In practice this proved to be an optimistic forecast because creep of the resin encasing the copper wafer was of a similar order as that of the salt. The result was equilibrium at a much lower pressure than the predicted in situ pressure.

Pressure cells provided useful information on the distribution of stress in the salt surrounding the excavation despite reaching equilibrium at a low pressure. Figure 4.7 and 4.8 show the pressure distributions in the floor and west wall of the drift respectively. All cells were measuring circumferential pressures except for the 3 m L (floor) and 15 m L (wall) cells which measured pressure along the axis of the drift. The 15 m wall cell was re-pressured to 15.5 MPa after 80 days in an attempt to measure the true in situ stress. It reached equilibrium at a pressure 11.6 Mpa. After one year it was again pressured to 15.5 Mpa and again stabilized at 11.6 Mpa. The perpendicular 15 m L cell was also repressured but it failed soon afterwards.

Corrosion of the stainless steel pressure tubing resulted in a number of cells failing after approximately one year. In future, cells used in wet conditions will be installed in oil filled boreholes and with plastic coated tubing from the hole to

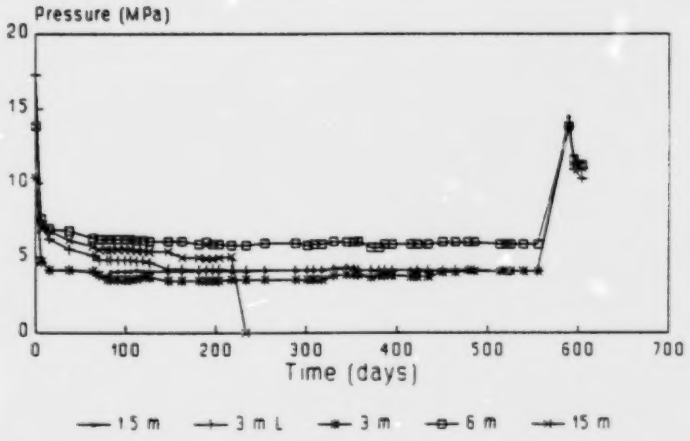

Figure 4.7 Pressure cell readings in the floor of the rock mechanics room

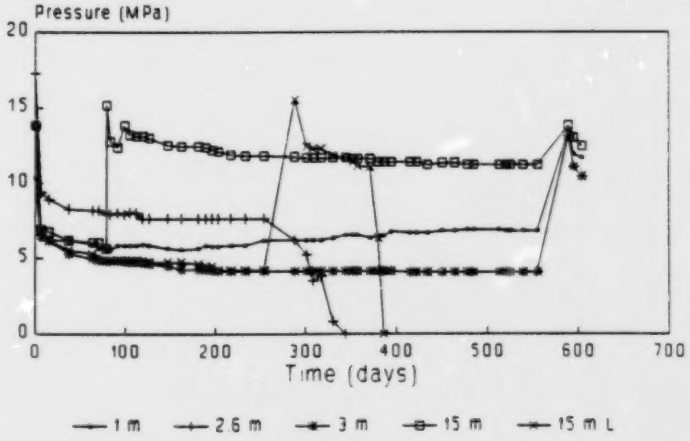

Figure 4.8 Pressure cell readings in the west wall of the rock mechanics room

the gauge.

A in the 189+00 diamond drill cross-cut on the 1850 exploration level was also instrumented with closure points and extensometers. The cross cut was 9 m x 3 m high and at the same depth as the cross cut discussed above. Half of the 80 m length of this excavation was in potash and half in the Upper Halite. Closure rates in the Upper Halite matched those in the 178+00 cross-cut once the different geometry was accounted for. They are compared to the potash closure rates in section 4.3.3. Extensometer readings are plotted in Fig 4.9. The very low deformation rates have resulted in somewhat erratic response from the extensometers; the extensometer rods are fairly heavy and corrode slightly in the holes which probably results in a certain amount of stick-slip movement. Extensometers show approximately 50% of the total wall movement takes place in the first 1.5 m and 90% or more in the first 6 m.

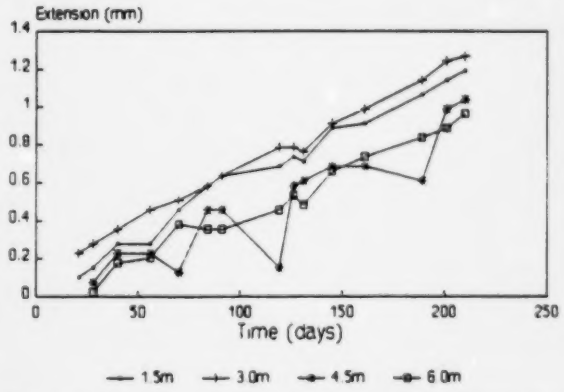

Figure 4.9 Extensometer measurements from the Upper Halite, 189+00 cross cut

Deformation measurements indicate clearly that the Upper Halite is the least mobile of the evaporite strata exposed in the mine at low stresses and is probably also most likely to behave in a brittle manner at higher stresses.

Numerical modelling of these drifts for the purpose of verifying visco-elastic material properties is reported in Chapter 6.

4.2.2 Middle Halite

In Middle Halite there was no need to develop openings especially for rock mechanics measurements since there are numerous cross cuts between the main entry system and the potash stopes. These are all of a moderate size and are well isolated from other large excavations. Typical cross-cuts are 11.5 m wide and 3.6 m high. Most are approximately 100 m long.

The cross cut to the 1500-2 east tailings ramps was instrumented with total horizontal closure points and rod extensometers in the wall; closure of several other ramp cross cuts was also monitored. All the instrument locations were between 550 m and 565 m below surface. Closure of the cross cuts reaches a steady rate of 0.075 mm to .1 mm per day

within a few months of mining. Horizontal deformations are limited to within 6 m of the excavation walls. It is clear from the Figures that the creep rate in the Middle Halite is considerably greater than that in the Upper Halite.

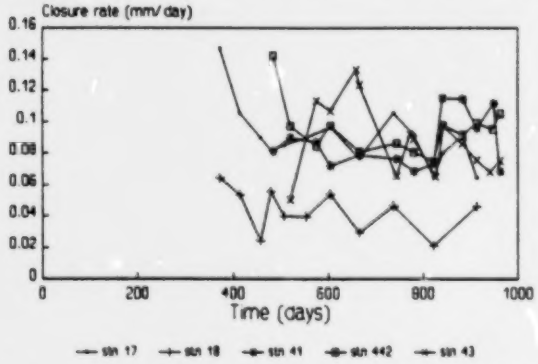

Figure 4.10 Closure rates of cross cuts in the Middle Halite

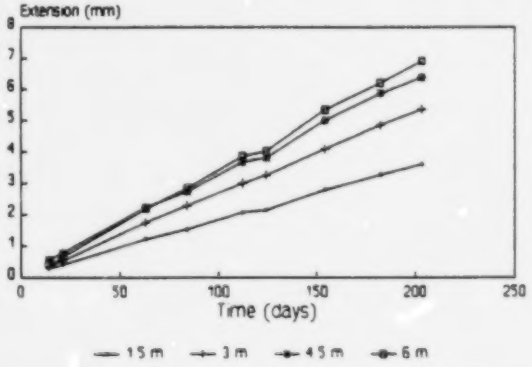

Figure 4.11 Extensometer measurements in the 1500-2 east tailings cross cut (station 33)

A number of closure points placed in the workshop area of the shaft pillar also registered steady closure rates of 0.075 mm per day. The extraction ratio in the workshop area is approximately 40% over a 60 m x 300 m area and typical excavations are 8 m x 3 m high.

4.2.3 Basal Halite

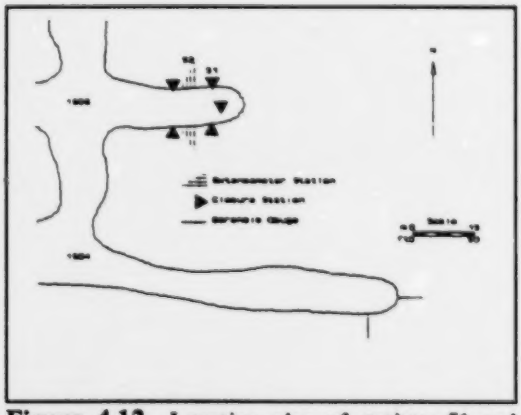

Figure 4.12 Location plan of stations 51 and 52 in the Basal Halite, 1900 level main entry

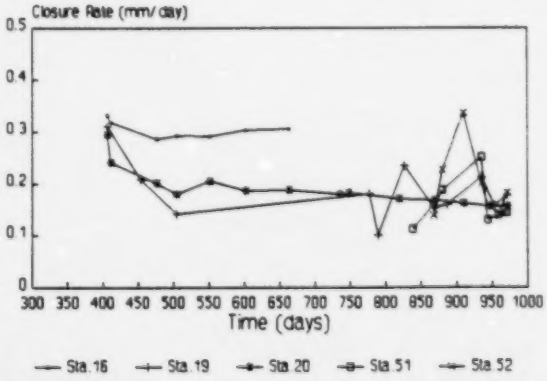

Figure 4.13 Closure rates at various points along 1906 main entry.

All instrumentation in the Basal Halite was placed in the 1900 level main entry system and the salt stopes. The entries represent a geometrically simple excavation in which instrumentation results are easily interpreted. By installing instruments ahead of salt stope development, measurements could be made before the additional stresses imposed by mining were experienced. Closure points were installed at several locations along the 1906 drift, as indicated in Figure 2.5. These points permitted comparison between stope proximity and closure rate which could be used to study the sensitivity of creep rate to stress.

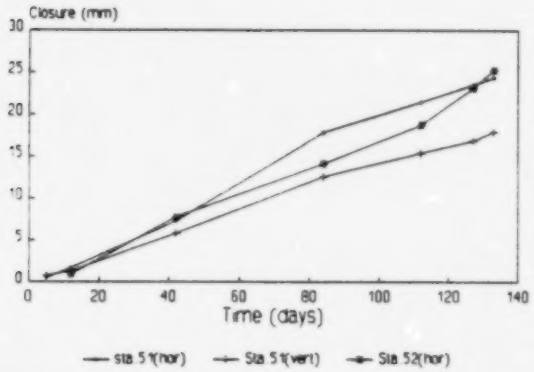

Figure 4.14 Total closures in the Basal Halite at stations 51 and 52

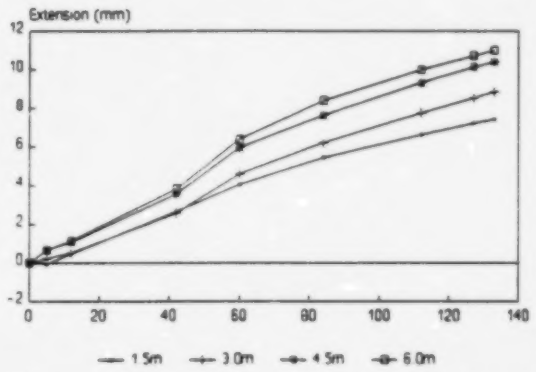

Figure 4.15 Extensometer readings from north wall at station 52, Basal Halite

Closure stations were placed 1 month to 2 years after mining and station 16 in particular missed most of the transient ceep. Stations 16 and 20 are only 40 m from the nearest salt stopes while station 19 is 120 m away. Both extensometers and closure points were placed at the end of the main entry, approximately 300 m from the nearest mining activity, as shown in Figure 4.12. The closure rate at this location was similar to that at station 19, suggesting that there is negligible effect on the main entry from the salt stoping at distances greater that 120 m. At stations which lie closer to the salt stoping, as shown in Figure 4.13, there is a clear effect on closure rate from the imposed abutment stresses. Extensometer readings and total horizontal and vertical closures are shown in Figures 4.14 and 4.15. Vertical closure of the 10 m x 3 m drift is approximately 75% of the horizontal closure. Extensometers indicate that 60% of the closure occurs in the first 1.5 m and 90% in the first 6 m of the walls.

4.2.4 Potash

Two entries on the 1850 exploration level and one on the lower stope sill cut elevation (703 m below surface) were instrumented with extensometers and closure points.

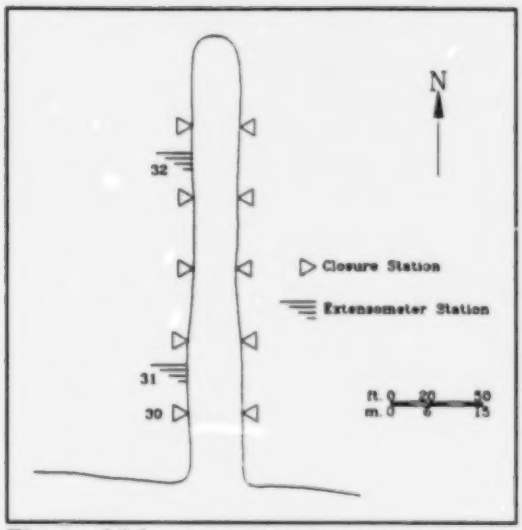

Figure 4.16 Instrumentation layout in the 189+00 cross cut

The 189+00 diamond drill cross cut is an interesting site because it is driven through both Potash and Upper Halite. This has permitted direct comparison between their deformation characteristics. Figure 4.17 shows the total closures measured at 12 m intervals along the cross cut. Closure stations were installed 120 days after excavation. Clearly there is a trend towards decreasing closures with increasing distances from the exploration drift. Superimposed on that trend there is a significant difference in closure rate between the salt and potash. An acceleration in closure between 50 and 100 days was caused by mining of a ramp 12 m below station 1 in the 189+00 cross cut. The effect of mining this small ramp was observable at all of the stations, which are up to 60 m away. However, it apparantly had no long term influence; stations 1, 2 and 3, which are at increasing distances from the ramp all have similar closure rates after 300 days. Modelling, which is discussed in Chapter 6, supports the observation that the only significant impact of the ramp is an immediate elastic deformation.

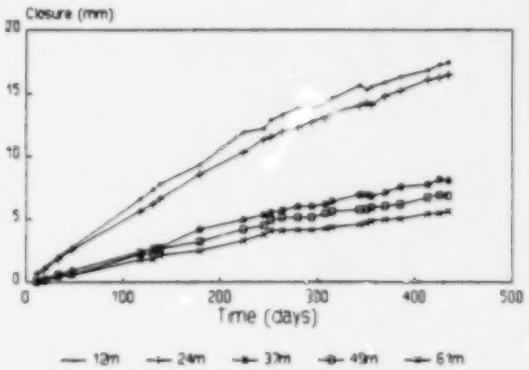

Figure 4.17 Total closures measured in potash and salt in 189+00 cross cut

Steady state closure rates in the potash drifts are approximately 2.5 x 10^{-3} mm per day. 50% of the deformation responsible for the drift closure occurs within 1.5 m of the wall and 90 % occurs within 6 m. Extensometer movements shown in Figure 4.18 display some of the stick-slip motion observed in other locations and it is probable that corrosion and dial gauge misalignment are responsible.

4.3 Instrumentation of Stopes

4.3.1 1900-2 Potash Stope.

To provide verification of the validity of extrapolating the results of measurements of small

drifts to the prediction of stope behaviour, detailed monitoring of a potash stope was carried out. The 1900-2 stope was chosen as a compromise between the rate of mining (the rate at which data could be collected) and ease of access for installing and monitoring the instrumentation. A section at the location is shown in Figure 4.19.

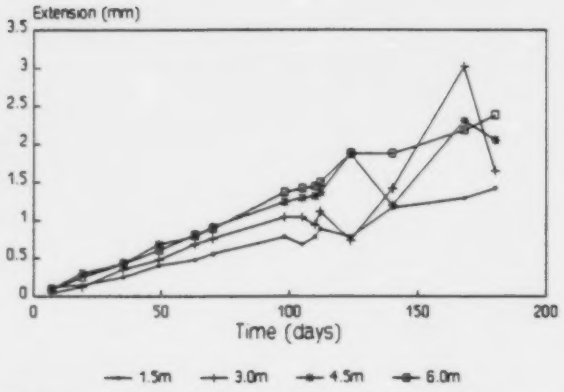

Figure 4.18 Extensometer readings in Potash in the 189+00 cross cut

The intent was to monitor deformations in and around the stope and the pressure being exerted upon the salt backfill by the stope walls. This amount of information is sufficient to confirm the validity of a modelling approach based upon results from small drifts. Instruments have been installed on two levels in the stope and will be added on at least one more level before the stope is completed. This will result in a complete picture of stope deformations

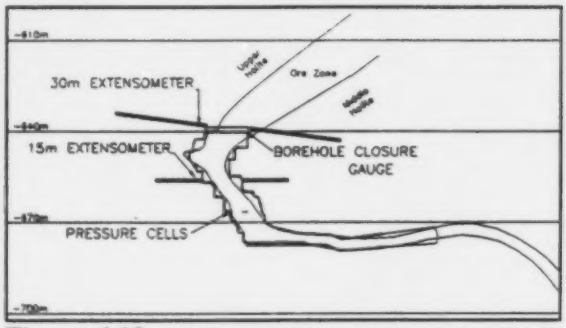

Figure 4.19 Instrumentation layout at 140+00 section of 1900-2 stope

On the 4th lift of the stope (elevation -632.6 m, section 140+00) 15 m long, 5 point extensometers were installed in the hanging wall and footwall. Four earth pressure cells were positioned to measure the pressure at the wall-fill interface and the vertical and lateral pressure in the middle of the stope. Cables for remote reading were run to the centre ore ramp.

On the 10th lift of the stope (elevation -603.6 m, section 136+00) a similar system was installed. Extensometers were 30 m long and the lateral earth pressure cell in the centre of the stope was omitted. A total closure COR-P gauge was added. Again, all instrumentation cables were run to the centre ore ramp.

4.3.1.1 Earth Pressure Cells

Earth pressure cell results from the 4th lift are shown in Fig. 4.20. Seven 4 m thick lifts of fill were added during the period covered by the data and there are corresponding peaks in the footwall pressure cell readings. The time of mining of a new lift is generally within a few days of placement of the fill. The measured vertical pressure remained almost constant after three lifts of fill had been added, indicating that arching between the walls is an important mechanism. The pressure on the overturned hanging wall increased

steadily for five lifts but has levelled at about 70% of the vertical pressure. On the footwall the pressure has risen in a very erratic manner. This is believed to be a result of cycles of slumping (rotational shear failure) of fill into the gap under the footwall, followed by shrinkage. Each of the pressure increases has coincided with the addition of new fill and the passing of the mining machine above the cell location. The maximum support pressure of 100 kPa is consistent with predictions of pressures in a loose, compressible fill. Lateral pressure measurements can be used to calculate the 'at-rest' earth pressure coefficient and hence the angle of internal friction of the fill. Calculated in this way the angle of internal friction is 44°. The apparent rise in internal friction with time may have resulted from shrinkage of the fill in the lateral direction - 44° should be viewed as the upper limit of friction angle while the lower limit is 30° which was calculated after 2 lifts of fill had been placed over the cells.

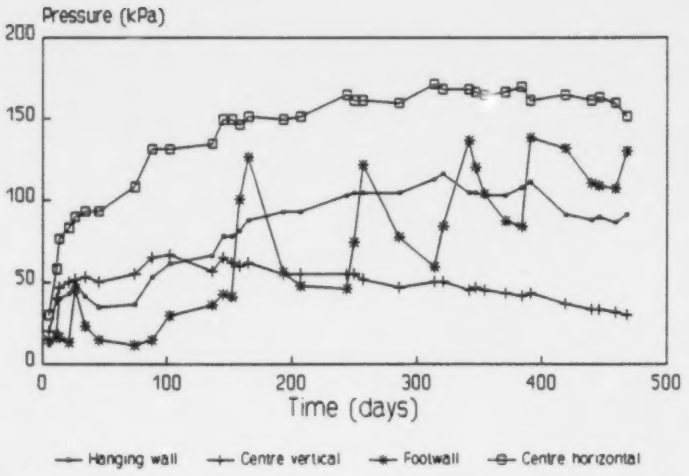

Figure 4.20 Earth pressure cell readings from lift 4 of 1900-2 stope

It is probable that the hard layers of drier and more compact material on the surface of each layer acts as reinforcement which give the fill a greater ability to arch between the walls than would be the case for the uniform material modelled. The effect of arching is to reduce fill pressures below the full overburden pressure. Voids which are left against the walls during filling of some areas which may cause low or irregular pressures.

4.3.1.2 Multi-point extensometers

Extensometers installed on the 4th lift in the footwall and the 5th lift in the hanging wall have anchors located at depths of 3 m, 6 m, 9 m, 12 m, and 15 m. Several observations result from study of the measured deformations shown in Figures 4.21 and 4.22. The first is that in both the hanging wall and the footwall the deformations extend well beyond the deepest anchor. The strain in successive 3 m sections of borehole is of similar magnitude rather than decaying to zero as it would at the farthest extent of deformation. Next,it will be observed that the footwall deformations are only one third of the hanging wall deformations despite clear indications elsewhere that the Middle Halite creeps more rapidly than the Upper Halite. In the footwall, the strain in the first 3 m of wall is negative. Both of these anomalies were found to be caused by the stope geometry and

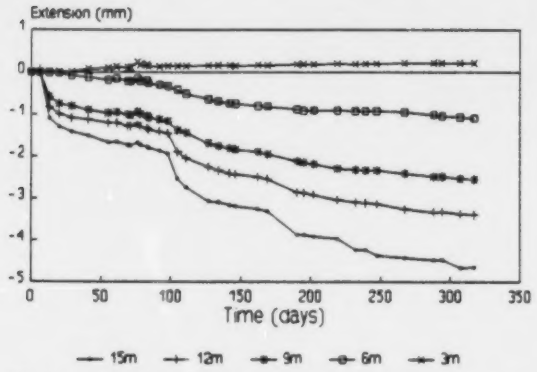

Figure 4.21 Extensometer readings from the footwall of 1900-2 stope, 4th lift

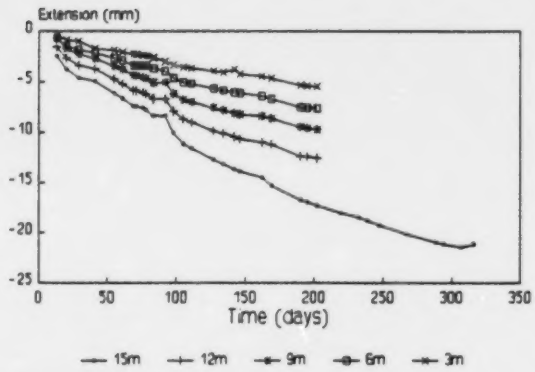

Figure 4.22 Extensometer readings from the hanging wall of 1900-2 stope, 5th lift

were explained by visco-elastic computer modelling. The footwall extensometer is in a very lightly stressed area in which creep rates are low. Creep of the folded footwall into the excavation results in extension and thinning of the wall surface and negative strains perpendicular to the wall. Destressing is extensive in the hanging wall and it may be accompanied by bed separation. Observable deformations were predicted by modelling to extend to at least 30 m.

A cable failure in the hanging wall extensometer resulted in the loss of all but the deepest anchor after 200 days, although contact with these anchors has now been re-established.

4.3.1.3 Closures

Closures have been monitored on each lift since the third lift. The locations measured have been predominantly in steeply dipping parts of the ore because of the instability of the hanging wall experienced in less steep areas. Closure rates have increased approximately linearly with increasing stope height, as shown by Figure 4.23. There is some indication that the initial closure rate following mining increases with stope height faster than the steady state rate. This result might be expected if it is assumed that creep rate is a nonlinear function of stress at high stresses and a nearly linear function at lower stresses. Thus, immediately after cutting, when there is a high stress concentration in the back of the

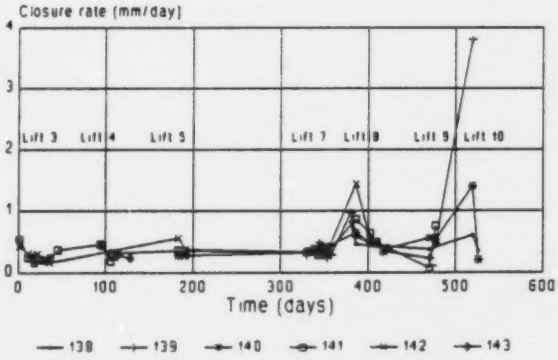

Figure 4.23 Closure rates on successive lifts of the 1900-2 stope (legend numbers indicate mine sections)

stope, there is a high rate of closure. However, as the stresses redistribute they return to the linear range.

Closures on the open lift obviously represent the lower limit of closures within the stope. At the middle of the open span greater closure rates were anticipated due to both stress relief creep and bed separation. The COR-P gauge was installed at the middle of the anticipated stope height to measure the maximum closure. At the time of writing it is only 2 lifts below the open lift (15 m below the crown) so the values measured do not represent the current maximum stope closures and are not reported here.

4.3.2 Salt stopes

Closure rates are being monitored in several salt stopes to verify the scale effects which were predicted from modelling. Closure of the salt stopes is important in itself because they are designed for permanent liquid storage and significant volume loss will have a negative impact on their functionality. The behaviour of the salt stopes also has a critical effect on the stability of the main entries and the response of the entries to stope mining is being monitored as part of the design process. Insufficent data has ben collected to date to date to report here.

4.3.3 Salt Pillars

The behaviour of pillars received relatively little attention until the end of this programme because of the limited requirement for pillar design optimization in the current mine layout. However, pressure to improve the extraction ratio in the high grade Basal Halite close to the main entry drifts is likely to increase the demands placed on pillars in the future. As a result it is important to begin monitoring the performance of pillars where they do exist to provide a basis for future designs.

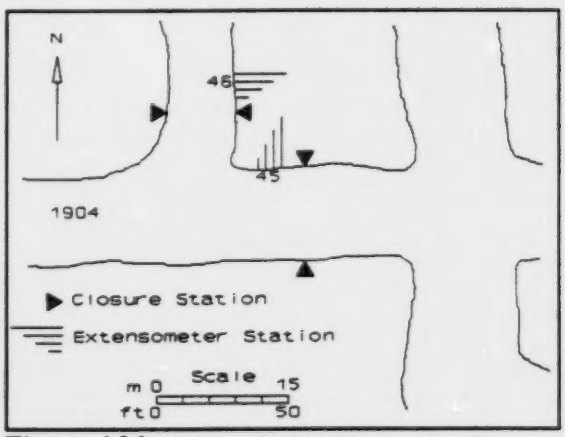

Figure 4.24 Instrumentation layout at main entry cross cut intersection at 172+50

Figure 4.24 shows the location of an instrumented pillar on the 1900 level main entry. Referring to Figure 2.5, it can be seen that this location is only 20 m from a salt stope, to which much of the damage is attributable. Figures 4.25 and 4.26 demonstrate that pillar deformation is predominantly in a direction perpendicular to the entries. A

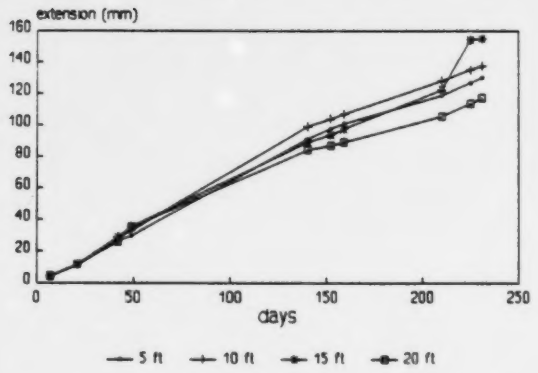

Figure 4.25 Expansions in the south wall of salt pillar

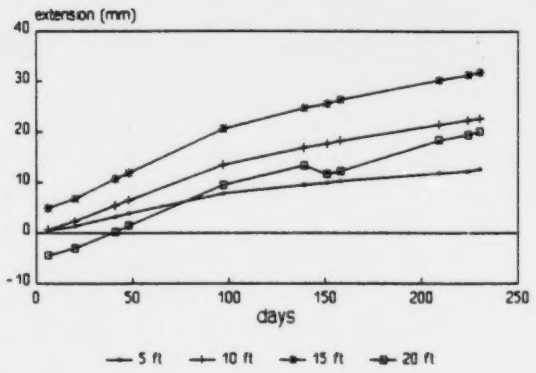

Figure 4.26 Expansions in the west wall of salt pillar

majority of the wall expansion on the south wall is within 1.5 m of the face, indicating that shear failure has caused separation of a block which is sliding or buckling into the opening. Buckling is visible in situ. Minor differences between extensometers can be accounted for by the fact that they are placed in individual holes approximately 0.5 m apart. It has generally been found that failure occurs in the walls of the drifts but not in the 25 to 30 m long cross cuts. This is the case whether the pillars are square or rectangular.

No separation has occurred in the west wall, where deformation rates are presumably within the secondary (or steady state) creep limit of the salt. The creep rate observed up to 100 days was $6.1 \cdot 10^{-10}$ /second and it then decreased to $2.4 \cdot 10^{-10}$/second.

4.4 Discussion

Instrumentation in the mine was designed to satisfy two objectives. The first was to provide information on the response of each of the evaporite strata to applied stress for comparison with laboratory test results and numerical model predictions. The second was to provide wide coverage of the mine with simple closure stations to establish a baseline of data with which future measurements could be compared.

The plan for the first objective was to begin in areas in which there would be little ambiguity in the results and from there to progress to the more complex stoping areas, collecting sufficient information to gain confidence in the numerical models. Without such an orderly progression, there would certainly have been resources wasted by installing and monitoring instruments in locations where they were ineffective or where the interpretation of results would have been in error.

Instruments were chosen for their simplicity and robustness since they had to operate in

a corrosive environment, often buried in tailings. Remote data acquisition was only used for buried instruments. Although instruments elsewhere could have been automated and the data collected centrally or transferred through telephone lines the benefits of regular visits to all areas of the mine by rock mechanics personnel outweighed the disadvantages. Routine, direct observation of ground conditions and interaction with mine workers yielded both technical and morale benefits.

Closure stations measured with a tape extensometer were the most widely used instrumentation, followed by rod extensometers. Both were inexpensive and sensitive. Commercial multi-point extensometers from ROCTEST and earth pressure cells from GEOKON both worked well, though the GEOKON equipment had clear superiority in terms of ruggedness and was thus more reliable. Borehole pressure cells proved to be inaccurate and tests of various designs of hydraulic wafer and cylindrical cells are continuing. Adequate cells are probably available commercially though the high cost of those reviewed precluded purchasing a sufficient number to give useful results. A borehole closure device with data logger is the most recent addition to the range of instrumentation and while this has not been fully tested it offers considerable promise.

Comparison of total closure rates indicated that creep of the Upper Halite was much slower than any of the lower evaporites. Potash and Middle Halite crept at approximately twice the rate and the Basal Halite at three to four times the rate under similar conditions. The Potash and Upper and Middle Halites creep at a slightly slower rate than comparable rocks in Saskatchewan and, of course, the mining depth is much less which has caused some difficulties in the transfer of instrumentation technology from that area. For each material approximately 90% of the closure was accounted for by deformations in the first 6 m of the walls, while 50% occurred in the first 1.5 m. In the potash stope, the slow creep rate of the Upper Halite appears to result in high stress concentrations and brittle deformations. Extensometers suggest the possibility of fracturing extending upwards of 15 m into the hanging wall. In Basal Halite, the rapid creep rate results in stopes which are highly stable in the short term, allowing large caverns to be mined very rapidly without artificial support. The negative side of this behaviour can be felt in the permanent entries which are influenced by stoping at a considerable distance and consequently suffer damage from high closure rates.

The baseline data which has been collected provides a viable method of assessing the success of new designs and the accuracy of the numerical simulations. Safety related installations such as short extensometers for monitoring back movements in the travelways also benefit from the existence of long term deformation measurements against which comparisons can be made and which will eventually form the basis of performance and safety criteria.

The determination of the pre-mining in situ stress field is one task which remains incomplete and it is one on which some effort must be expended in the future. Pressure

cells in the Upper Halite have given some indication that the horizontal stresses are between 80 and 100% of the vertical overburden stress. This is realistic when compared to other measurements in Eastern Canada. The traditional hard rock methods of stress measurement such as the doorstopper and hollow inclusion gauges were avoided because of doubts about the reliability of data interpretation in salt. In the near future the problem will be addressed using the CANMET borehole gauges.

There is always the need for more economical and more reliable instruments which can cope with the rigors of the mine environment. Specific needs are improved borehole pressure cells and more reliable, waterproof, long stroke, electronic extensometer heads. A project currently being carried out in conjunction with CANMET to develop buried radio transmitters capable of transmitting instrument data through fill will, if successful, solve many of the problems currently associated with cabled data acquisition.

5. Laboratory testing

5.1 Introduction

Laboratory testing plays an important part in establishing the mechanical properties of a rock mass. However, laboratory tests of evaporites have often been criticized for the poor approximation they give to in situ conditions. It is true that data scatter for many tests is greater than for other rock types and that mechanical properties derived from tests are commonly at odds with those derived from in situ tests or derived from back calculation of in situ measurements. However, laboratory tests provide the only effective method of subjecting the rock to a range of stress paths under accurately known boundary conditions. Establishing even semi-quantitative relationships between applied stress and mechanical properties is of sufficient importance to justify a laboratory testing programme.

All testing of intact evaporites was carried out by the WATSALT facility at the University of Waterloo. The WATSALT laboratory is equipped to perform triaxial and uniaxial strength tests and confined creep tests on 100 mm diameter core samples. Its innovative equipment is well suited to evaporite testing.

Laboratory tests were not performed on salt tailings backfill because it was not possible to obtain the undisturbed samples which are required for meaningful testing. Numerous studies of the properties of reconstituted samples are reported in the literature and these were referred to when an approximate constitutive law was needed; the literature is discussed later in this Chapter. It is hoped that sampling and in situ testing of consolidated tailings can be accomplished in the future.

Testing of borehole pressure cells was undertaken in a bench scale test apparatus at the mine after it was realized that the borehole pressure cells installed at the beginning of the project were ineffective. Several types of soft inclusion cell were tested and the results are reported here.

5.2 Core Sampling and Sample Description

Intact rock samples were recovered using a 100 mm diameter double tube core barrel powered by a Longyear diamond drill. Although not ideal, saturated brine was used as the drilling fluid. Samples were carefully dried immediately after removal from the core tube and sealed in wax. All core recovered from the first 6 m of each hole was presumed to be affected in some detrimental way by mining and was discarded.

Basal Halite was sampled from a horizontal borehole in the shaft pillar at mine coordinates 102000N, 8500E. The core was almost pure NaCl with less than 1% anhydrite impurities. The salt crystals were anhedral, being between 2 mm and 4 mm in diameter

and 10 mm long.

Upper Halite and Potash were sampled from horizontal boreholes in the 189+00 cross cut on the 1850 Exploration level. The fine grained Upper Halite contained approximately 2% clay impurities and occasional discrete anhydrite laminae. The samples were taken approximately perpendicular to the bedding. Distinct orange, brown and clear beds could be observed. The Potash contained 45 % KCl and approximately 2% anhydrite; the remainder was halite. The crystals range from 1 mm to about 20 mm in maximum dimension, though are predominantly below 5 mm. Their shape was generally anhedral and tabular, often giving the core a schistose appearance. Slickensided shears are commonly found in the ore zone but were not observed in the core. A significant proportion of the halite (up to 10 %) was dark blue; this is believed to be indicative of high stresses. While the blue halite follows the schistose fabric the crystals are euhedral. They often surround larger sylvite and halite crystals, giving a reticulate appearance perpendicular to the schistosity.

Samples were packed in a two component expanded rubber foam for shipment to Waterloo. Laboratory core logs indicate that they generally arrived in good condition but some loss of bonding of the wax was noted which possibly resulted in changes to the surface moisture content.

5.3 Laboratory Facilities

The following descriptions of laboratory equipment and procedures are extracted from a report presented to PCA by the University of Waterloo. That report (Fordham and Dusseault, 1988, 1989) is available upon request. Much of the information is also contained in other references, to which the reader is referred (Dusseault et al., 1985 and Baleshta and Dusseault, 1988).

Triaxial tests were performed on 102 mm diameter samples using a modified Hoek cell arrangement. The test cell differs from the standard Hoek cell in its urethane membrane/seal design and by having a closed reaction cap as one end rather than a second loading platten. Axial strain measurement is by external LVDTs mounted between the loading piston and the reaction cap platten of the triaxial cell.

Creep tests were performed using totally self-contained triaxial testing systems in which the axial load piston forms the lower platten. The sample is contained in a urethane jacket which also serves as the oil seal for the confining pressure system in the same way as the cell mentioned above. This innovative design is well suited to creep tests in which rapid piston movements are not required. Pressure control is by microprocessor controlled accumulator-intensifiers using nitrogen cylinders as the low pressure supply. A data acquisition system records pressures and piston movement. The stress on the sample is

determined from the oil pressure by calibrations performed with load cells and axial deformation is assumed to be the same as piston movement. Strains are calculated from the actual sample length at the time of the measurement. The minimum measurable strain rate is approximately $5 \cdot 10^{-10}$/s.

Temperatures can be controlled from room temperature to about 50°C using insulated covers for the cells equipped with a heat source (light bulbs), a fan and a thermistor. The fan and lights are under microprocessor control and can maintain a temperature to within ±0.1°. An attempt was made to maintain a temperature of 18°C for the PCA tests but fluctuations of the laboratory temperature made this impossible and the idea was abandoned in favour of a 23°C standard.

5.4 Test procedures

Samples were cut to a height/diameter ratio of 2.0 and the ends dry ground using 600 grit. The loading plattens were sprayed with a dry lubricant to minimize end restraint.

To reverse some of the effects of sampling-induced stress relief, samples were hydrostatically consolidated at 20 MPa for 3 to 5 days prior to creep testing. Creep tests were then begun by dropping the confining pressure to the desired level for the first load stage. Each stage was maintained for approximately three weeks, including at least 7 days of 'steady state' creep. The creep at the end of the load stage was taken as the steady state rate for that shear stress. The load was then adjusted to begin a new stage. Up to 6 load stages per sample were applied. Loads were adjusted to give increasing, decreasing or constant shear stress in order to explore a range of load paths.

Triaxial strength tests were performed at confining pressures of 1, 2 and 3 MPa. The load was applied at a constant strain rate of 10^{-4}/second. One unload-reload cycle was performed for the determination of the static tangent Young's modulus.

Brazilian tests were performed on 54 mm thick discs of core, loaded by curved platens across their diameter. An indirect tensile strength can be determined from the load at which the disc splits.

Dynamic elastic moduli were determined by sonic velocity according to ASTM D 2845-83. Dynamic tests provide the benefit of removing the influence of creep upon the apparent elastic strain which is present in load tests, but the validity of moduli determined in this way has never been demonstrated in practice. The difficulty of measuring the shear wave velocity in these tests necessitated using an assumed Poisson's ratio for the calculation of Young's modulus. This, of course, introduces a further source of error into the results.

5.5 Intact Material Test Results

5.5.1 Brittle Yield Tests

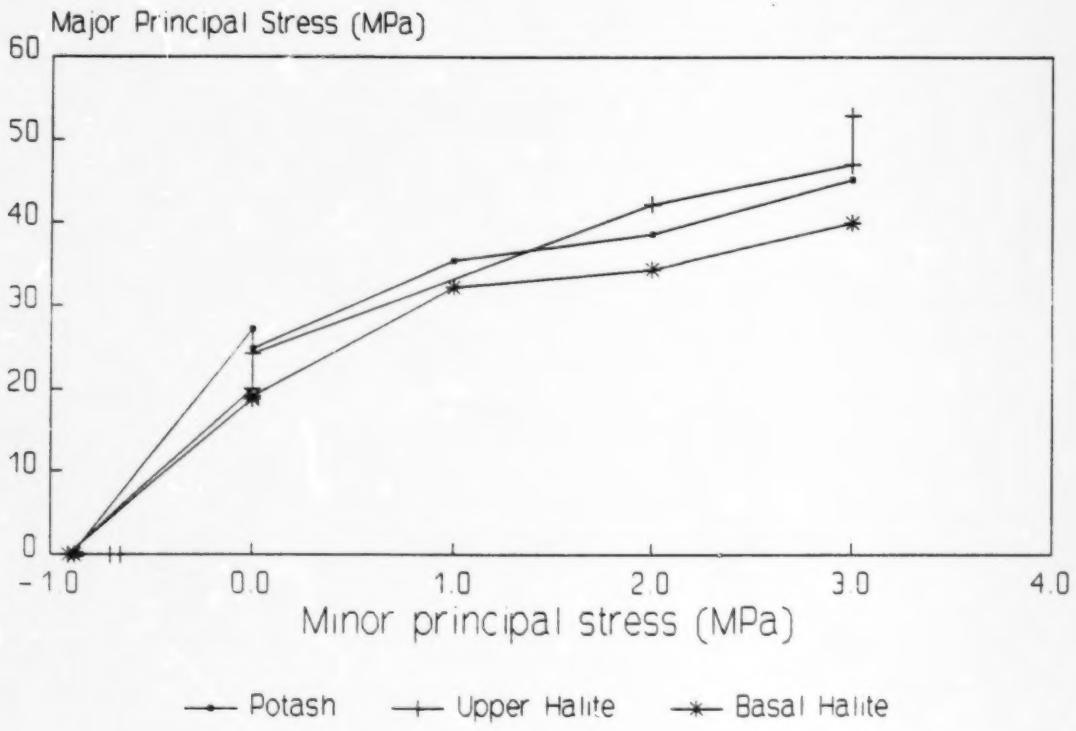

Figure 5.1 Failure stress states in brittle yield tests

The results of the entire series of brittle yield tests are shown in Figure 5.1. The results were fitted to three failure envelopes - a Rothenburg criterion, a Hoek-Brown criterion and a Mohr-Coulomb criterion. The three criteria are:

Rothenburg: $\sigma_1 = \sigma_c/2[(1\text{-}RM) + [(1+RM)^2 + 4M(\sigma_3/\sigma_c)]^{1/2}]$

Hoek-Brown: $\sigma_1 = \sigma_3 + (mo_c\sigma_3 + s\sigma_c^2)^{1/2}$

Mohr-Coulomb: $T = c + \sigma_n \sin\phi$

where: σ_1 = major principal stress
σ_3 = minor principal stress

σ_n = normal stress on shear plane
σ_c = unconfined compressive strength
ø = angle of internal friction
R = σ_c/σ_T
M,m and s are constants

The values determined for these and other elastic constants are given in Table 4.1. Poisson's ratio is assumed to be constant for all materials. A value of 0.33 has been assumed for calculation of the dynamic modulus although 0.3 has been used for most of the modelling work. Literature values typically vary from 0.25 to 0.35.

Table 5.1 Elastic constants and strength envelope parameters for PCA evaporites

Material	E	E_d	σ_c	σ_T	c	ø	m	s	M
Upper Halite	5.67	27.62	22	.75	4	52	24	.5	35
Middle* Halite	6.9		28	1.48	4	58			34
Basal Halite	7.56	29.75	19	.9	5	37	18	.5	33
Potash	6.62	14.93	26	.87	7	40	13	.5	22

* From Denison-Potacan (1987)
Strength values in MPa, Young's modulus values in GPa

Both the Rothenburg and Hoek-Brown criteria are non-linear strength envelopes, which is a clear advantage for evaporites in which the non-linearity is very marked. Both give reasonable fits for the small range of confining stresses used in the laboratory tests but have doubtful applicability much beyond that range because the salt yields too rapidly to fail in a brittle manner. The envelope should in reality level off more rapidly than either criterion. A second difficulty is that neither criterion has a plastic flow rule and thus cannot be implemented in an elasto-plastic numerical scheme. They are therefore useful for identifying regions of failure in an elastic model such as EXAMINE (a boundary element program discussed in Chapter 6) but cannot be used in more sophisticated models in which load redistribution occurs following local yielding as the stress state in the yielded

material is returned to the yield or residual strength envelope.

The Mohr-Coulomb criterion offers the advantage of a reliable flow rule at the expense of a linear failure envelope which probably grossly over-estimates strength at high confining stresses. The term 'strength' used in this sense includes both brittle yield and very rapid creep because excessive flow is tantamount to failure in many practical applications and its effect on load redistribution is similar. Although the combination of a Mohr-Coulomb criterion and a suitable creep law can be used effectively in many cases, the analyst must be aware of the limitations of criterion and interpret his results with care.

The dynamic moduli are significantly greater than moduli measured from load testing. They are close to values often quoted in the literature for halite (25 - 30 GPa) and the in situ values possibly lie between the direct and dynamic determinations. Directly measured moduli were used for most of the modelling referred to in this report but there are some indications that these values are rather low.

5.5.2 Physical properties

Table 5.2 gives the measured density and moisture content of the materials tested. Some error in moisture content may have been introduced by wet coring, although the results are believed to be accurate. The higher moisture content in the Basal Halite may be the cause of its high creep rate relative to that of Upper Halite which has been observed in the mine. Moisture at grain boundaries is thought to facilitate creep by a mechanism of pressure solution.

Table 5.2 Physical properties of PCA evaporites

Material	Moisture Content %	Density g/cc
Upper Halite	0.01	2.13
Basal Halite	0.35	2.15
Potash	0.29	2.12

5.5.3 Creep tests

Creep tests were performed on the Upper and Basal Halites and Potash. The primary aim of the testing programme was to accurately define the relationship between steady state creep and applied stress. Shear stress level is the dominant factor in determining isothermal creep, but the effect of varying the normal stress level was also investigated. An attempt was made to determine the activation energy of the materials by constant stress/variable temperature tests.

Multiple load stage tests have not been widely used in the past for evaporite testing but

their validity for determining steady state creep rates can be defended. Transient creep can be considered to be an exhaustion process (Day, 1985) in which, for a given energy applied to the system, creep centres will activate, or cause strain, and then require a much greater energy input to reactivate. Assuming there are a finite number of these creep centres, the process will eventually be exhausted and no further creep will take place. If this theory is accepted, a multi-stage test will produce quite different transient creep at a given stress level than would a single stage test at the same stress. However, steady state creep is by definition an inexhaustible process and should thus be identical at a given stress, independent of the load path of the sample.

Displacement-time curves for the salts tested are presented on the following page. The numbers at each step in the curve represent the axial and confining stress for that load step. The slope of a tangent to the curve at the end of the load step was taken as the

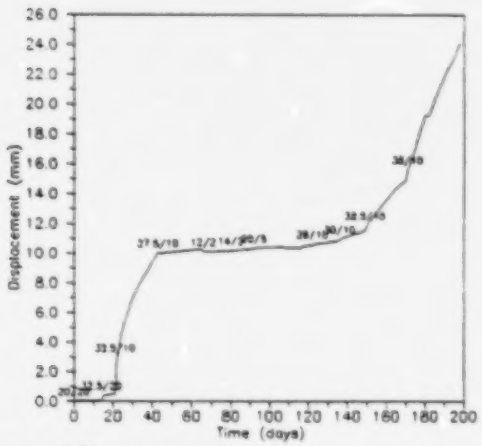

Figure 5.2 Potash sample P11

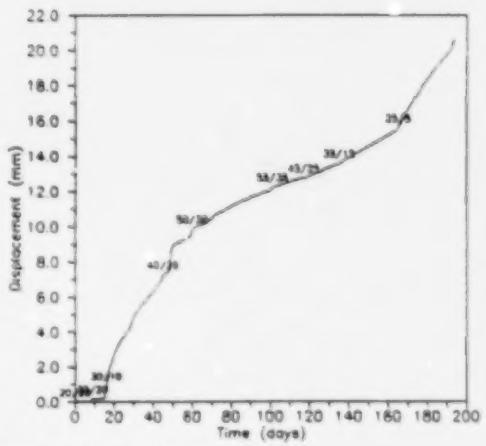

Figure 5.3 Potash sample P18

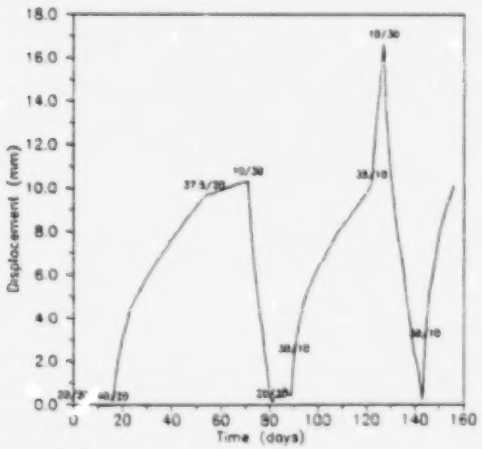

Figure 5.4 Potash sample P216A

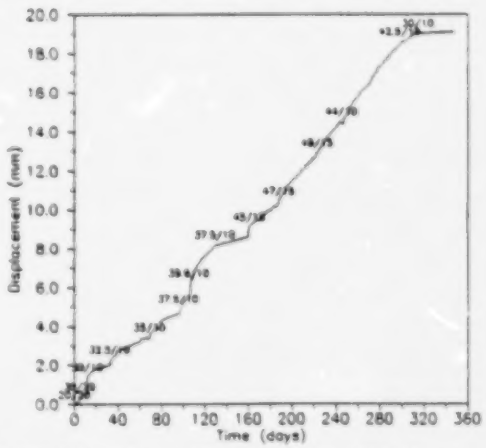

Figure 5.5 Upper Halite sample UH40A

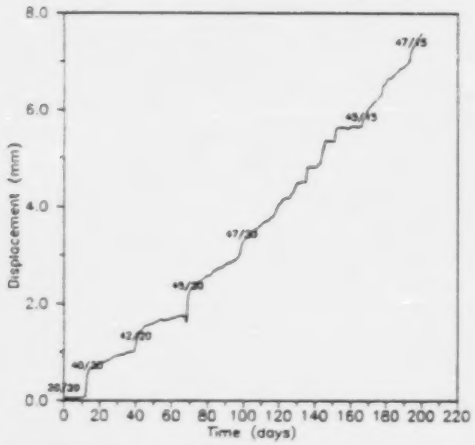

Figure 5.6 Upper Halite sample UH2730B

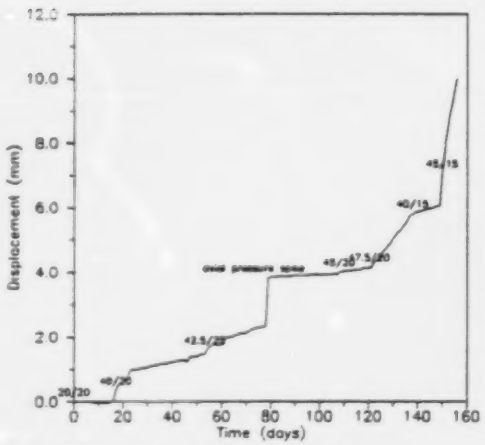

Figure 5.7 Basal Halite sample LH1516

steady state creep rate for that load. These rates were used for deriving the creep parameters presented in the following section.

Potash sample P18 was tested at constant shear stress (o_1-o_3=20MPa) but over a range of mean stresses. The influence of mean stress on creep rate has been discounted or ignored in most creep formulations but it was believed to be worthwhile quantifying its importance in this study. Figure 5.8 compares steady state creep rates to mean stress ((o_1+o_3)/2). Some effect is evident from the Figure; a regression analysis yielded the relationship:

$$\dot{e} = 2.13 \cdot 10^{-7}\ \sigma_n^{-1.22} \quad \text{for constant shear stress at } 18^{\circ}C$$

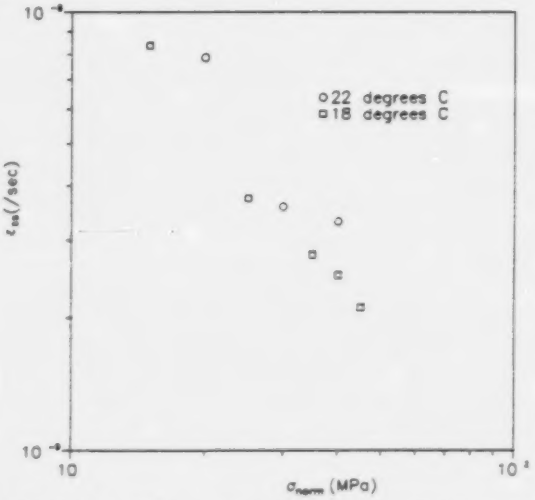

Figure 5.8 Mean stress effects on the creep rate of Potash

While the mean stress effect appears to be demonstrated by these results it is probably not of sufficient importance to be an essential component of a constitutive law covering the small range of mean stress with which this mine is concerned.

The apparent activation energy, Q_a, was calculated from changes in creep rate resulting from a 3°C change in temperature during tests of Potash and Upper Halite. The temperature change is rather too small to obtain a reliable value but the attempt is worthwhile because the value of exp(-Q/RT), where R is the gas constant and T is

temperature in Kelvin, is needed in several creep models. Values of 15.3 and 2.2 kcal/mol were obtained for Potash and Upper Halite respectively. The former is reasonable but the latter much lower than literature values.

5.5.4 Creep models proposed

Material models, or constitutive laws, are mathematical idealizations of material behaviour which allow numerical analyses of the response of a system to applied loads and displacements. The familiar Hooke's Law (Extension = K x Load) for the extension of a spring is a simple example. For the case of creep of evaporites it is necessary to introduce time as a variable and account for the non-linearity of the stress-displacement rate curve. Creep is a complex combination of mechanisms which is by no means thoroughly understood and the relationship between the constitutive laws and the physics of those mechanisms is rather tenuous. A law must be chosen with reference to conditions which must be simulated. For instance, temperature variation is minimal in the PCA mine so accurate modelling of temperature effects is superfluous.

The creep laws presented here are derived from a combination of the results of laboratory tests and comparisons between computer models and in situ measurements. In general, stress dependency is obtained from laboratory tests and other constants from field data analysis or literature.

A power law, in which the strain rate is related to stress raised to some power is the basis of most steady state constitutive laws. However, the laboratory tests provide some support for the thesis, proposed by Dusseault et al. (1987), that there is an increase in the exponent as stress increases and that a bi-linear power law is appropriate. The law has been stated in different ways but takes the form:

$$\dot{e} = \dot{e}_{crit}[(\sigma_1-\sigma_3)/\sigma_{crit}]^n \qquad \text{for } \sigma_1-\sigma_3 > \sigma_{crit}$$

$$\dot{e} = \dot{e}_{crit}[(\sigma_1-\sigma_3)/\sigma_{crit}]^m \qquad \text{for } \sigma_1-\sigma_3 < \sigma_{crit}$$

where: $\dot{e}_{crit}$ is the strain rate at the critical shear stress
σ_{crit} is the difference between minimum and maximum principal stress at which a change from a low rate to a high rate mechanism takes place

A single stage power law is sufficient for a majority of analyses in which shear stresses are not large enough to trigger the higher rate creep mechanism. Since it was easier to match a single stage law to field data, the fits were often better. In addition, the standard creep version of FLAC contains a reliable steady state power law (the WIPP law) but not the bilinear law. The form of the law is:

$$\dot{e} = A \cdot \sigma^{p} \cdot \exp(-Q/RT)$$

where: σ is $\sqrt{3}\sqrt{J_2}$ where J_2 is the second invariant of deviator stress
Q is activation energy
R is the gas constant
T is the temperature if Kelvin
A and p are empirical fitting paramters

The constants determined for these two laws from laboratory tests are given in Table 5.3. The constants A and $\dot{e}_{crit}$ are not given reliably by laboratory tests and must be

Table 5.3 Creep law constants for PCA evaporites

Material	m	n	σ_{crit}	$\dot{e}_{crit}$	A	Q/R	p
Upper Halite	2	4.32	25	$2 \cdot 10^{-11*}$	$2.7 \cdot 10^{-4}$	6060^{+}	2
Middle Halite	1^{*}	4.8^{+}	18.8^{+}	$4 \cdot 10^{-11*}$	$8.6 \cdot 10\text{-}^{4}$	6060^{+}	2
Basal Halite	1^{*}	4.25	12.72	$6 \cdot 10^{-11*}$	$2.37 \cdot 10^{-3}$	6060^{+}	2
Potash	1^{*}	8.75	17.47	$2 \cdot 10^{-11*}$	0.16	7777	2

$^{+}$ Literature values
* Values derived from comparison between models and field data

determined from an analysis of steady state field data. Comparisons between models using these constitutive laws and field data are given in Chapter 6.

5.6 Backfill material model

The response of salt backfill to stress is extremely complex. Densification occurs as a result of consolidation, salt grain creep, pressure solution/reprecipitation and dessication. The importance of these mechanisms depends upon the initial density, moisture content and stress level. However, since the function of the fill is to provide support to the stope walls and to the mining machines, its most important properties are its stiffness and the shear strength at the exposed surface. Stiffness is shown here to be primarily a function of voids ratio which, in the mining context, is controlled by the degree of stope closure for

a given initial density. The material model described is based upon testing reported in the literature; tailings studies were not incorporated into the Rock Mechanics Programme.

The particle size distribution for the run-of-mill tailings is shown in Figure 5.9. The gradation corresponds to a poorly graded fine sand with a coefficient of uniformity

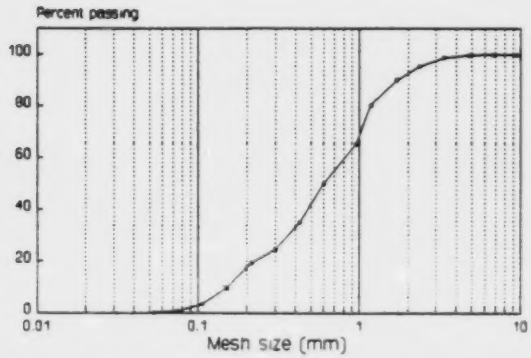

Figure 5.9 Particle size distribution for mine tailings

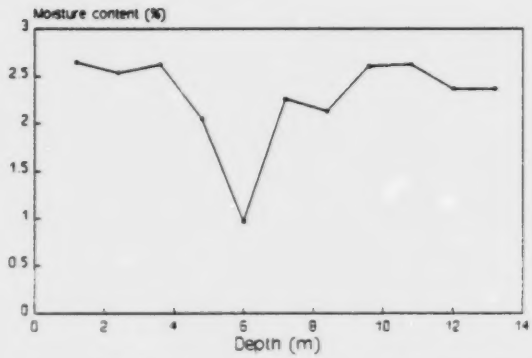

Figure 5.10 Moisture content in a vertical section of fill 6-12 months old

(D_{60}/D_{10}) of 4.8. The moisture content at the time of placement is 6-8% but the brine drains rapidly to leave a moisture content of about 2%. Figure 5.10 shows the distribution of moisture content in tailings which have been in place between 6 and 10 months. The density of placed tailings depends upon the location within the stope cross-section; the maximum is about 1600 kg/m3 near the centre line and it decreases to 1400 kg/m3 at the walls.

5.6.1 Literature review.

The behaviour of salt tailings has received attention in several countries due to its importance in the proposed disposal of nuclear waste in salt deposits. Numerous laboratory studies of the consolidation and strength development of fine salt under a variety of load and moisture conditions have been performed. Several studies (e.g. Pfeifle et al. (1984), Hesterman (1979))have shown that the degree of consolidation achieved during loading is dependent upon the maximum stress and time under load. The presence of moisture is important in facilitating consolidation, possibly because pressure solution is a contributing mechanism. However, the results of Miller (1983) suggest that the actual moisture content may be of secondary importance. Strength development is strongly influenced by time under load; a sample which was quasi-statically loaded to 21 MPa possessed no strength (Holcomb and Hannum, 1982) whereas one consolidated for three weeks under the same load achieved an unconfined strength of 11 MPa (Beddoes, 1984). The importance of secondary crystal growth during the period of creep in the development

of strength was shown qualitatively in electron micrographs by Beddoes (ibid).

Based upon laboratory testing, relationships between creep rate, stress, time and porosity (Korthaus, 1984) and between bulk modulus and stress (Holcomb and Hannum, 1982) have been proposed. They each have limitations in describing in situ behaviour where load controlled conditions do not prevail.

Studies of the in situ characteristics of salt tailings are limited and provide little guidance for design purposes. Kappei and Gessler (1984) have reported on the deformation and permeability of 60 year old fill. Although it contained other industrial wastes which have unknown influence, a cohesion of 1 MPa had developed and the angle of internal friction was 60°. Distinct consolidation was noted during creep tests of recovered core despite the length of time over which the fill had been subjected to rock loads from stope closure.

The application of salt backfill for strata support in potash mining has become a topic of concern in Saskatchewan, where longwall mining methods have been considered, and in New Brunswick, where high extraction mining is practised. However, the studies thus far published have been of insufficient scope to yield useful information on in situ fill properties and the long term support it might provide.

5.6.2 Proposed Material Model

Of primary importance is the compressibility, or bulk modulus, of the backfill. Since the fill is completely confined within the stope, its ability to withstand shear stress (its 'strength') is of little concern. Study of the results of consolidation, creep and strength tests on tailings from a Saskatchewan mine (Beddoes, 1984) led to the conclusion that, independent of initial density, maximum stress or time under load, bulk modulus could be

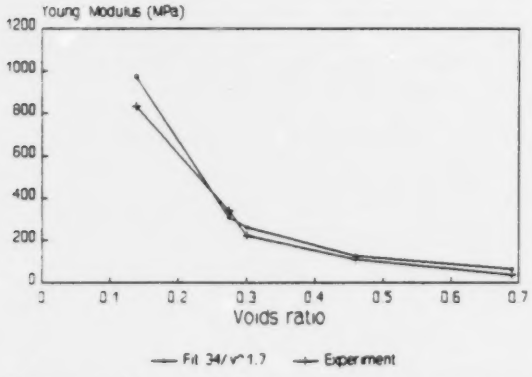

Figure 5.11 Comparison between proposed model and experimental data

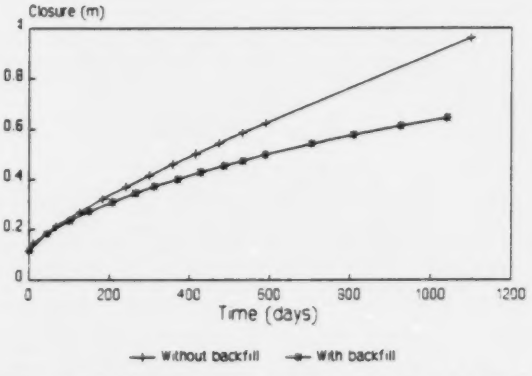

Figure 5.12 Comparison between closure of filled and unfilled salt stopes

related to void ratio (v = Vol. voids/Vol. solids) A relationship between Young's modulus and void ratio, assuming a constant Poisson's ratio of 0.28, was formulated from this data. Young's, rather than bulk, modulus was used for the sake of convenience in the computer implementation. The form of the relationship is:

$$E = 34/v^{1.7} \text{ MPa}$$

Figure 5.11 compares this relationship with the laboratory data. Although all the other material models in GEOROC are visco-elastic, omitting the time variable from the backfill model is felt to be justified because the rate of deformation of the fill will always be controlled by the rate of closure of the stope.

5.6.3 Computer implementation

The model can be readily implemented in a finite element program because the volume of every element is calculated routinely, thus the void ratio at any time can be found if its value at the time of placement is known. In order to reduce the number of times which the stiffness matrix must be recalculated as the fill becomes stiffer, a user-specified ratio between the newly calculated and previous stiffness must be exceeded. This value is normally set at 1.1. In addition, the fill stiffness is checked before being updated to ensure that it has not exceeded that of the host salt.

Figure 5.12 illustrates the typical effect of backfill, described by the proposed relationship, upon the closure of a long cavity with a 25 m x 15 m high cross-section. Such an excavation is typical of the salt stoping area of the PCA mine. Closure of this stope in the highly plastic Basal Halite is effectively halted within 5 years provided the cavity is tightly filled at an initial density of 1600 kg/m^3.

5.7 Laboratory Testing of Pressure Cells

As discussed in Chapter 4, the Saskatchewan Research Council pressure cells installed in the rock mechanics room (178+00 cross cut) failed to react as predicted. It was assumed that, given the simple geometry and geology of the test site, the cells were more likely to be in error than the predictions. As a result, a simple series of tests on the SRC designs of copper wafer cells were carried out.

Denison-Potacan (1987) established that the cells correctly registered pressures applied to them by a triaxial loading system. However, the loading system used was an infinitely soft one (i.e. the applied loads remained constant irrespective of the strain within the pressure cell). This is not representative of the in situ state, in which the loading applied to the cell is strain rate limited (the load cannot be applied faster than the strain rate of the salt

under the existing shear stress). This difference in loading conditions becomes extremely important if any part of the pressure cell system also creeps when loaded. Having hypothesized that the resin encasing the pressure cells was able to creep at a rate which was significant in comparison to the creep rate of salt, a test series was designed.

Two steel cylinders were fabricated according to the design in Figure 5.13. Dial gauges could be mounted on the ends of the cylinders to measure the extension of the pressure cell inside them. Pressure cells were tested by inserting them in the cylinders, pressurizing them to a predetermined pressure, then closing the hydraulic circuit with a valve. The pressure was then read regularly until it had stabilized. A second pressure increment was then applied and the procedure repeated. Longitudinal cell extension in several tests was measured with dial gauges.

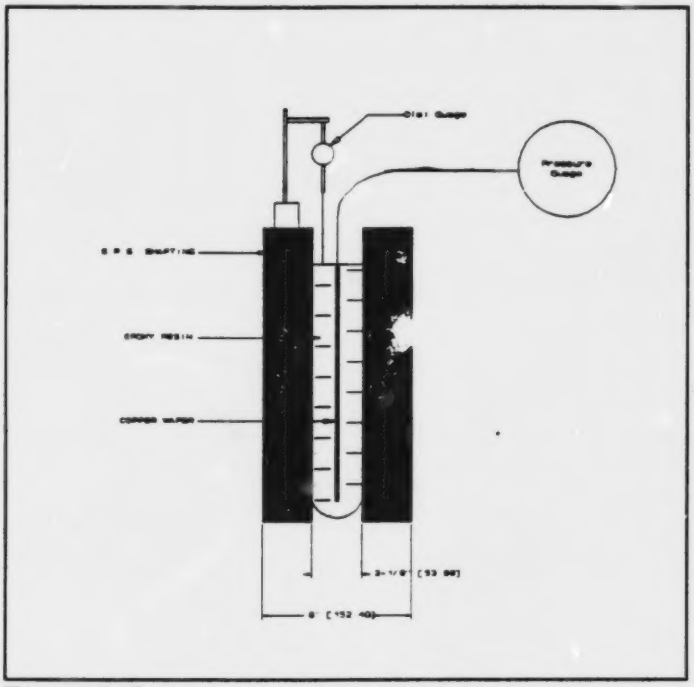

Figure 5.13 Pressure cell test apparatus

Cells encased in resin (Sika Dur), potash and ciment fondu grout were tested in this manner. A series of pressures which covered the range of pressure expected in the rock mass (8.5 to 21 MPa) were used for each. Figure 5.14 shows a typical pressure-time curve for a resin encased cell. The pressure dropped very rapidly to 30 to 50% of its set pressure and then stabilized to a constant pressure. Some work hardening appears to take place as the pressure loss on the first pressure increment was much greater than that on subsequent increments. Re-pressuring the system to the same pressure on successive increments resulted in a higher stable pressure. Measurements of longitudinal extension indicated that the pressure loss was accompanied by extrusion of the casing material out of the end of the cylinder.

The potash encased cell lost 34 to 40% of the set pressure on each increment. Longitudinal extensions were not detectable. The large oscillations about the steady state pressure shown in Figure 5.15 were caused by temperature variations in the room of up to 10°C. The cement and resin encased cells were not sensitive to temperature variations.

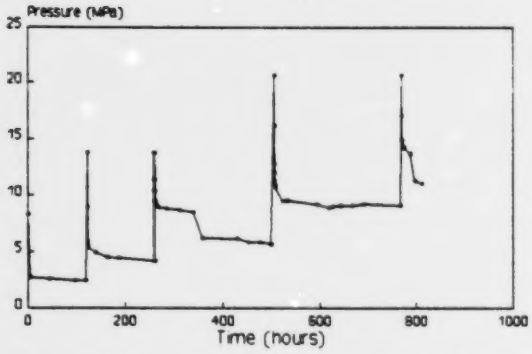

Figure 5.14 Pressure-time response of resin encased cell

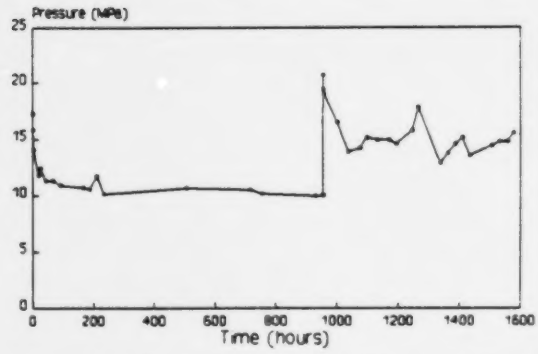

Figure 5.15 Pressure time response of potash encased cell

Ciment fondu was chosen for an encasing material because it reaches its ultimate compressive strength very rapidly and is chemically resistant. The grout mix contained 1.3:1 sand:cement and 0.44:1 water:cement ratios. The moulded cell was cured for 7 days prior to loading it in the test cylinder. Cement encased cells proved to be the most stable of the three types tested. The pressure drops on each load increment were 32 % of the setting pressure which was the least of all the cells tested. Little sensitivity to temperature variations was observed and the longitudinal extension was below measurable limits.

Based upon these tests, a resin encased cell appears to be a poor choice for pressure measurement in a location with a very low creep rate. The very low steady state pressures recorded in the rock mechanics room clearly result from the rapid creep of the encasing resin. If a pressure cell is to record a correct pressure it must creep at a lower rate than the surrounding rock mass. A cell made from the same material as the rock mass will necessarily read a lower pressure than the in situ pressure. Due to the lack of restraint on the end of the cell, the shear stress in the cell is higher than in the rock surrounding the borehole resulting in a higher creep rate.

Subsequent tests conducted in Middle Halite in the shaft pillar confirmed that the cement grout encased cell gave higher stable pressure readings than cells encased in potash or resin.

5.8 Discussion

Laboratory tests were performed on intact core samples of Potash, Upper and Basal Halite at the University of Waterloo. Determination of the time dependent properties of the evaporites was the primary concern although a series of triaxial brittle yield tests were also performed in each rock type. The Waterloo laboratory is the best equipped in Canada for the type of testing required.

Creep tests were performed on a small number of samples with multiple load stages. The testing procedure is based upon the assumption that steady state creep is attained within one to two weeks and that the steady state creep rate is unaffected by the load path of of specimen. Neither assumption has been thoroughly validated but the approximation is sufficiently good to allow meaningful relationships between applied stress and creep rate to be derived.

There was a close similarity between the strengths and elastic properties of the different rock types. Uniaxial compressive strengths lay between 19 MPa for the Basal Halite and 26 MPa for the Potash, a range which is in accordance with other evaporites in the literature. Young's moduli, which were obtained from one unload-reload cycle, are lower than values quoted in the literature by a factor of two to three. They range from 5.7 GPa for the Upper Halite to 7.5 GPa for the Basal Halite. It is tempting to explain low modulus values in terms of the inelastic strain occurring during loading or sampling induced damage but a clear case cannot be made for either explanation here and the results appear to fit reasonably well with field data.

Several useful observations can be made regarding the creep tests. The first is that the Upper Halite samples give an indication of a change of stress exponent in the power law from 2 to 4.32 at a shear stress of 12.5 MPa. The higher exponent may actually be greater than quoted but reanalysis of the raw laboratory data is needed to prove this. Below a shear stress of 12.5 MPa the power law fit to the laboratory data is good and field data supports the stress exponent derived. The Basal Halite and Potash underwent much more rapid creep at the stress levels used for testing. The Basal Halite had a stress exponent of 4.25 for the shear stresses used, which were all above 10 MPa. However, field data suggests that the exponent must reduce at lower shear stresses and is likely to be close to 2 below 6 MPa. The potash demonstrated very high stress dependency, giving a stress exponent of 8.5, but again field evidence is that stress dependency at lower stresses is greatly reduced.

The effect on creep rate of normal stress was investigated in one test. Although a minor effect was observed and quantified it was rather difficult to isolate that effect from others such as small temperature changes and the continuous slight decrease in strain rate with time which has been observed in other long term tests (e.g. Cominco, 1987). As a result it is felt that the inclusion of a normal stress effect in a constitutive law based upon a single test was unwarranted.

Steady state creep models were chosen for fitting to laboratory data for reasons of expediency. Steady state deformations represent the major proportions of total deformations in many practical instances. The relatively few parameters needed for the relevant laws can be obtained from fewer, shorter tests than would be needed to derive a suitable transient law. Finally, there is wide acceptance of the existence of steady state

creep and the form of the equation to describe it. There is compelling evidence from this project that there is not a unique relationship between stress and strain rate over the stress range up to yield and thus a bilinear law has been used to fit the data in addition to a simple power law. There is no clear evidence, however, that the bilinear simplification is justified. The stress exponent may well be a continuous function of stress.

Pressure cells of the type made by Saskatchewan Research Council were tested for pressure stability and it was found the epoxy resin encapsulating material underwent rapid transient creep and was thus unsuitable for use in locations where rapid creep was not expected. Cement encapsulation was found to give better stability while retaining the ease of fabrication of resin.

A review of salt tailings testing was made and a simple constitutive equation proposed. For the purposes of stope modelling, in which the tailings are loaded primarily by movements of the stope walls, an elastic model relating fill stiffness to voids ratio is felt to be adequate. Although creep consolidation will take place as an increment of displacement is applied, creep will have the effect of decreasing void ratio, making the fill stiffer when the next increment is applied. The only assumption which needs to be made is that the fill will creep very rapidly in comparison to the applied displacement rate, and that stresses will not build up without consolidation occurring. Observations indicate that this assumption is reasonable.

6. Numerical analysis and design

6.1 Introduction

The analysis and design component of the programme had two objectives. The first was to obtain and validate computer programs which were suitable for solving a wide range of problems encountered in mining in visco-plastic rocks. The second was to solve a number of problems which are of immediate importance to mine planning.

Although it was necessary to become involved in research oriented program development in some instances, the primary goal was to provide and validate methods which could be readily applied to practical problems by a user with limited rock mechanics and programming knowledge. Ease of use of the programs chosen became as important a criterion as their technical merit. It is our belief that this strategy provides the greatest long term benefit to the mine.

An attempt has been made to follow the advice of Starfield and Cundall (1988) in regard to the methodology of numerical modelling and design. Models often cannot be rigorously validated for the complex conditions found in mines, and instead it is necessary to use them for a wide range of problems and gain confidence in their ability to yield useful predictions. They may be used to gain insight into problems for which intuition alone, or in combination with instrumentation, is insufficient. A model should be as simple as possible while being consistent with the important features of the physical situation; unnecessary detail has a tendency to confuse the broader conclusions which can be drawn from the model. This is as true of the constitutive laws used to describe material behaviour as it is of the geometry of the model. Several different simple models often provide greater insight than does a single complex one. Finally, for the purpose of routine design it is often better to develop simple equations and guidelines from the model than to use the model itself directly as a design tool.

The intention throughout has been to progress from simple models of geometrically and geologically simple excavations to more rigorous models of realistic situations. For each type of rock in which mining takes place, small excavations have been modelled and the results compared to equivalent instrumented locations. Having validated material laws and computer models for these small scale problems, simulations of more complex excavations were performed and validated limited field measurements. Following this level of vailidation the models are ready to be used for trial designs and further validation can take place by monitoring the performance of excavations constructed according to the designs.

6.2 Computer codes

Modelling has been performed using several finite element, finite difference and boundary element programs, all of which have advantages and drawbacks. The features of these methods are described in standard texts such as Brady and Brown (1985) to which the reader interested in a comparison between them is referred. In general terms, the finite element and finite difference methods involve discretization of the problem domain into a number of elements for which equations of motion (in the case of the finite difference method) or force-displacement relationships (in the case of the finite element method) can be formulated and solved. Both methods allow for arbitrary geometry and complex stratigraphy to be modelled and are easily adapted to a variety of material constitutive relationships.

In contrast, the boundary element method, of which there are several variants, requires only that the boundary is discretized into linear elements. Integral equations relating the tractions on, and displacements of, each element are solved iteratively. The boundary element method offers advantages of great economy in formulating and solving a problem and in the realistic modelling of the 'infinite' extent of the rock mass. However, the features which result in its economy also make it less suitable for modelling heterogeneous rock masses and inelastic behaviour.

6.2.1 GEOROC

GEOROC is a finite element program, originally developed by RE/SPEC Inc. for U.S. nuclear waste disposal research, which was adapted for potash mining under contract to CANMET (Fossum et al, 1984). It is a visco-elastic model in which increments of viscous strain are calculated for a given stress from one of several available constitutive laws; the strains are then used as initial strains to update the nodal force vector. This in turn is used to recalculate the nodal displacements using a constant stiffnes matrix. New stresses are found by applying the material elasticity matrix and the process is repeated following the calculation of a stable time step.

Four non-linear material models are available in GEOROC. The most straightforward, and widely used, is the time power law:

$$e = A'\sigma^p t^q$$ where t=time

$\sigma = \sqrt{3}\sqrt{J_2}$

A',p and q are material constants. $A' = A \cdot \exp(-Q/RT)$ in terms of constants given in Table 5.3

The time power law can be reduced to the Norton steady state law by setting q=1. The second law is a bilinear power law proposed by Denison-Potacan (1987). Essentially, it is the same as the steady state form of the power law above, but the exponent p takes

different values, m and n, depending upon whether the principal stress difference is above or below a critical stress σ_{crit}, where $\sigma_{crit} = \sigma_1 - \sigma_3$. Normalized shear stress, $(\sigma_1 - \sigma_3)/\sigma_{crit}$ is substituted for σ in the power law equation. The critical shear stress, $\sigma_{crit}/2$, is assumed to be the shear stress at which a change in creep mechanism, from one which is diffusion controlled to one which is controlled by dislocation climb and glide, takes place. An exponent of 1.0 has been used for stresses below the critical stress.

The third law is based upon activation energy spectrum theory as developed by Day (1985). This treats transient creep as a probabilistic mechanism. An activation energy spectrum relates the material internal energy and the number of centres at which a creep event can take place. Various spectrum shapes can be used to model the response of different materials to applied stress. Creep in the model is a hyperbolic function of stress.

Lastly, a non-linear elastic model for consolidating backfill is included. This model has the form:

$$E = 34/v^{1.7} \qquad \text{where } v = \text{void ratio}$$

A non-linear elastic model was adopted for backfill for several reasons. There is a shortage of relevant laboratory tests on salt tailings due to the difficulty of obtaining undisturbed samples and reliable estimates of time dependent properties are not available. One of the few consistent properties found in long and short term laboratory tests is the relationship between stiffness and voids ratio (Beddoes, 1984). Such a relationship is relevant to cut and fill stoping because the main loading mechanism is stope closure is a rate controlled process. If the assumption is made that the tailings are much less stiff and will creep much more rapidly than the intact salt, the time dependent properties of the tailings are found to be insignificant.

GEOROC was used a great deal during the project because of the ease with which material property sensitivity analyses could be performed and because changes to the source code could readily be made. Most of the drifts and rooms which were monitored for the purpose of verifying material constitutive laws were small and lightly loaded. Therefore they behaved in a visco-elastic manner, without any visible damage, making them ideally suited to the capabilities of GEOROC. Material models were implemented and experimented with, providing insight into their validity and limitations.

6.2.2 FLAC

The finite difference program FLAC (Itasca Consulting Group, 1988) was bought in the latter part of the project for its ability to model visco-elastic and elasto-plastic materials and its high quality user interface. The belief that the long term needs of the mine are better served by a widely used commercial software package than by a research oriented program was also a motivating factor. FLAC contains a 2 stage transient/steady state

creep model developed for the WIPP[1] project and a classical Kelvin model. Mohr-Coulomb plasticity with or without tension cutoff, ubiquitous joint and structural models are also supported. These features suit the model to a wide variety of mining related problems.

FLAC was used for many of the large scale. or global, analyses in which failure and collapse were believed to be important mechanisms. It is far easier to model complex stratigraphy and excavation geometry with FLAC than with GEOROC (and most other finite element programs); this is a particularly important feature for modelling large scale problems.

6.2.3 Boundary element programs

A boundary element program based upon the coding presented in Hoek and Brown, 1980, was adapted for use in the early stages of the project. This was entirely adequate for analysis of any 2-dimensional, linear elastic problems but, like GEOROC, was somewhat limited in the flexibility of its pre- and post processing. Late in the project it was replaced by a similar program developed at the Universtity of Toronto. The latter has a user interface based on AutoCad and makes far better use of graphics and automated input generation.

Linear elastic programs have rather limited application to evaporite mining where there is both heterogeneity and material non-linearity. However, the insight they can provide into the mechanisms causing short-term instability caused by rapid mining advances can be of immense value. Investigation of the effect of changing the face cutting profile on hanging wall instability is one example of the application of the program. As a tool for routine interpretation of ground conditions the boundary element program has many advantages. Models are readily set up and the results easliy understood. Relatively little engineering judgement is required in choosing boundary and load conditions, making use of the program somewhat 'foolproof'.

6.3 Computer Hardware

At the beginning of the project a Compaq Deskpro 386 computer and peripheral devices were purchased. The computer was bought with a 130 Mb hard disk, 10 Mb of RAM and tape backup. A 80387 numeric coprocessor was added when it became available. Peripheral devices included a Houston Instrument DMP56C drum plotter, a Calcomp 9148

---

[1] Waste Isolation Pilot Project, an underground test facility in New Mexico used for nulclear waste disposal research

digitizer tablet and a Comrex line printer.

As processing requirements grew, a Compaq Deskpro 386/20e with a Weitek 3167 coprocessor was leased. The tripling of processing speed achieved by this machine made possible a series of very large non-linear models. A Hewlett-Packard Laserjet series II printer was also added to provide report quality print and graphics in 8½x11" format.

Some difficulties were experienced with the Compaq Deskpro 386 system in the early stages of the project, in large part because of the newness of the technology. Once reliable Fortran compilers became available and some hardware bugs were corrected the choice of equipment was vindicated. Currently, the Compaq computers are achieving turn-round times on numerical analyses which are competetive with mid range mini-computers. They are much better suited than the latter to a small mine engineering office where the overhead of maintaining a mini-computer would be onerous.

6.4 Material Property Validation

Numerical modelling requires that a reasonable approximation of the stress-strain-time relationships for the rock mass be determined. Laboratory testing is the first step in defining these relationships, but laboratory test samples invariably behave somewhat differently from the way in which the same material behaves in situ. As a result, the material properties determined in the laboratory often cannot be used directly for predictive modelling. Instead they must be verified, and adjusted as necessary, by modelling thoroughly instrumented excavations. The term 'verify' is used with some reservation; due to our limited knowledge of the mechanics of salt deformation under load it is, in general, not possible to model even a well posed problem with complete accuracy. A material model which appears to provide an exact fit to a test case may be very unreliable under other conditions. Rather than pursuing increasingly complex constitutive laws to produce improved accuracy it is often more productive to experiment with the model and gain a 'feel' for its limitations. Consequently, the approach taken here has been to choose relatively simple constitutive laws and test them for a wide range of cases for which field measurements are available.

Several test entries were created explicitly to obtain information suitable for comparison with the predictions of numerical models. These have been described in Chapter 4. Entries were monitored in Potash and Upper, Middle and Basal Halite using total closure stations and four point extensometers. In the case of the Upper Halite, oriented flat-jack pressure cells were also used. For each of these materials, approximate constitutive 'laws' were derived from the results of laboratory tests. This 'law' was then used as input in a simple GEOROC model of the entry. The mesh used for this model is illustrated in Fig. 6.1. In each case the entire rock mass within the zone of influence of the entry consists of one rock type. The model was rerun several times until a reasonable fit to at least two

sets of data had been achieved e.g. total closures and deformation distribution in the rib. The more sets of data that can be fitted, the more reliable will be the law that is eventually derived.

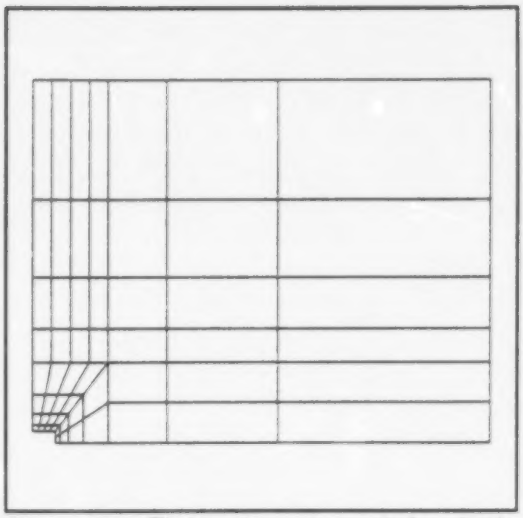

Figure 6.1 Finite element mesh for single drift calibration models

6.4.1 Upper Halite

Simulations of the rock mechanics room (178+00 cross cut) and the 189+00 cross cut were the matched with field data for the purpose of creep law validation. The values obtained from laboratory testing, and reproduced in Chapter 5, were used as first estimates for the creep constants. The stress exponents were maintained at the laboratory values while the coefficients in the constitutive laws were adjusted to optimize the fit to field data.

Inelastic closures predicted for the rock mechanics room are compared with field results in Figure 6.2 The field closure displays a high degree of transience which neither the power nor bilinear law match with great accuracy. The bilinear law provides the best fit to the steady state rate, although it is still an overestimate. The wall expansions (Figure 6.3) are best compared to readings in the 189+00 cross cut where extensometers were installed earlier and were more stable. The relationship between the wall expansion and the total closure is similar to the field results from which it has been observed that 6 m extensometers record approximately 90% of the total closure.

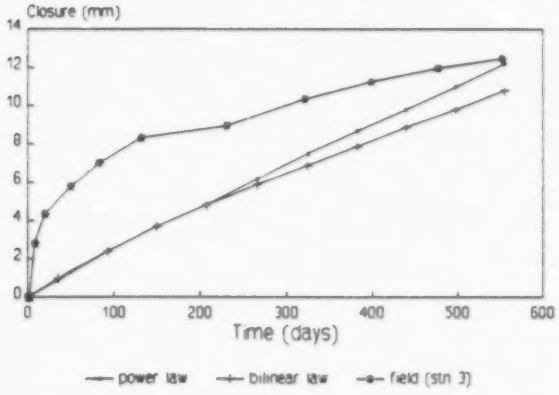

Figure 6.2 Predicted inelastic closures in the Rock Mechanics Room

Pressures predicted by the models are in marked disagreement with field data. It has been noted in Chapter 4 that the SRC pressure cells undergo significant creep which results in a pressure drop and eventual equilibrium at a pressure below the in situ pressure. It is encouraging, however, that the pressure distribution predicted by the models matches the measured distribution

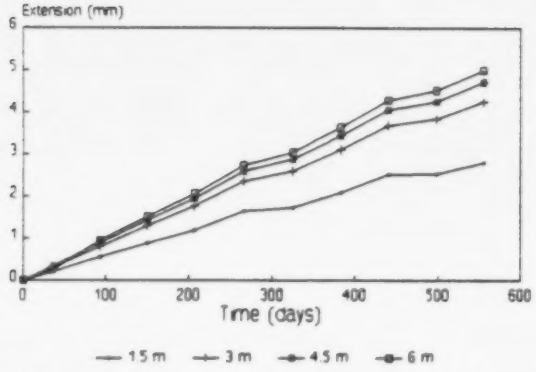

Figure 6.3 Predicted wall expansions in Upper Halite in the 189+00 cross cut

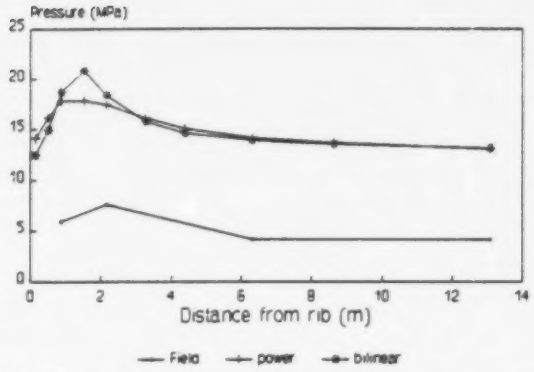

Figure 6.4 Predicted steady state pressure distributions in the wall of the Rock Mechanics Room

reasonably well. In Figure 6.4 the pressure peak predicted by the model appears to be rather closer to the excavation than the measured peak. The power law provides a better prediction of the peak pressure location because the higher stress exponent at low shear stresses causes more rapid stress redistribution. This is an indication that the stress dependence of strain rate below the critical shear stress may be underestimated in the bilinear law. The stress exponent is more likely to be around 2 rather than 1.

6.4.2 Middle Halite

Cross cuts from the 1900 level main entry to the potash stope ramps are the only access to Middle Halite apart from that provided in the shaft pillar. Several of these cross-cuts have been monitored for total horizontal closure. In addition, wall extensometers have been placed in the 1500-2 east tailings cross-cut and back extensometers have been placed in the 1900-3 centre ore cross-cut. Most of the instrumented locations are at least 70 m from the nearest excavation and 150 m from the nearest stoping operations.

Laboratory testing of Middle Halite was not undertaken so literature values for the stress exponent in the constitutive laws were used as a starting point in the calibration process. The constants proposed by Denison-Potacan were once again used in the bilinear law and exponents between 1.5 and 4 were used in the power lawbefore a value of 2 was chosen. Leading coefficients were readily determined for a given law because all excavations of 6 to 9 m wide by 3 to 4 m high have closed at a consistent ratc of .07 mm per day. Steady state closure has continued in several drifts for 18 months, confirming the existence of time-independent creep in the Penobsquis deposit.

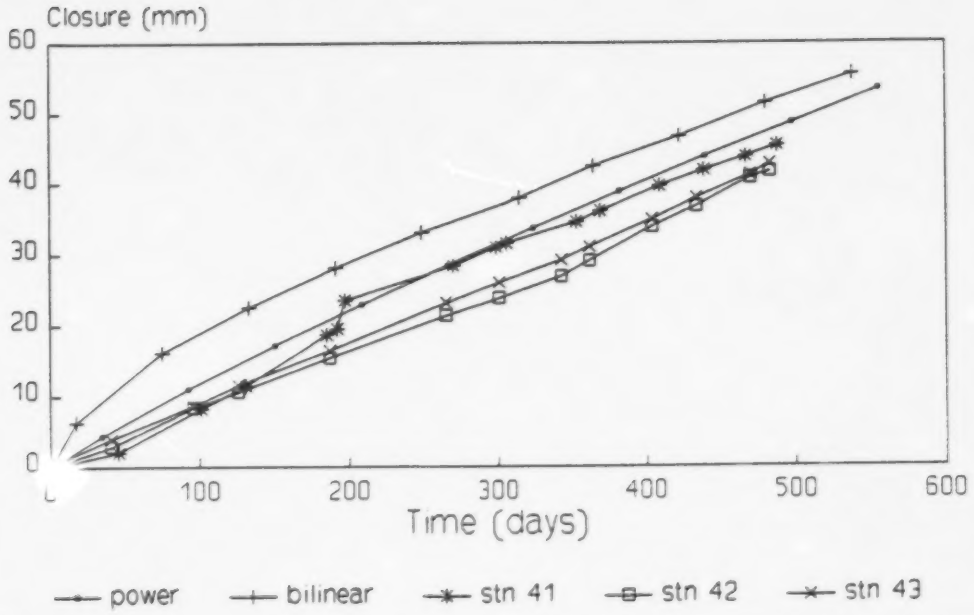

Figure 6.5 Total closures predicted by the power and bilinear laws compared to field measurements

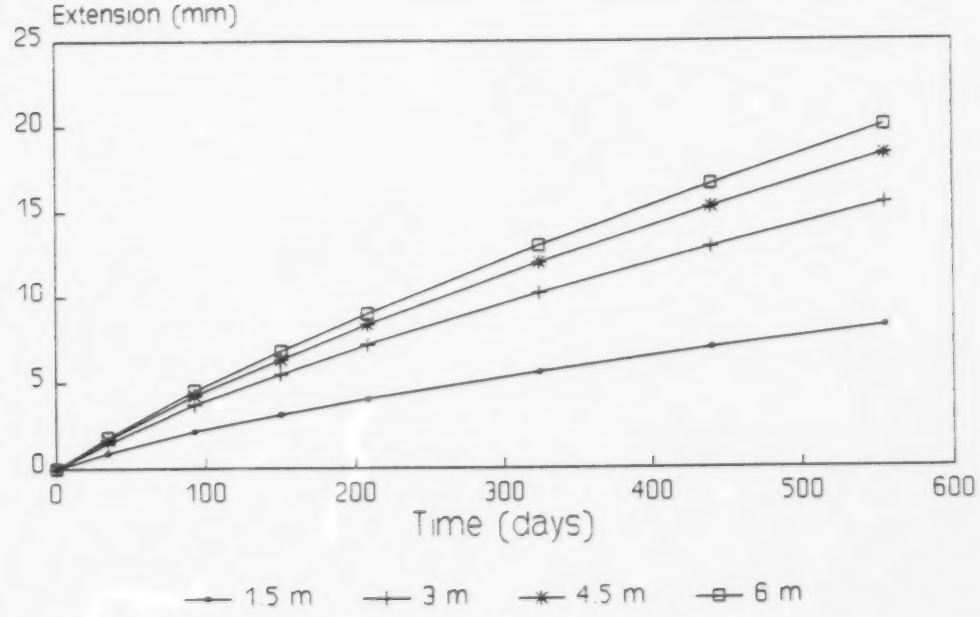

Figure 6.6 Predicted wall deformations using the bilinear power law

Both the single stage and bilinear power laws were able to match the closure rates after the initial transient period. As shown in Figure 6.5, the bilinear law matches the closure rate better than the power law after the transient stress redistribution stage. The transient stage, if it existed, was missed in the field monitoring which was begun several months after mining. The extensometer data was matched rather better by the single stage law. Figure 6.6, when compared to the field data in Figure 4.11, illustrates that modelling underestimated the deformation at the 6 m anchor by 10-15% and at the 1.5 m anchor by almost 50 %. This problem is observed commonly and its cause may be the presence of stress relief fractures close to the excavation wall. It may also be indicative of stress path dependence in the salt. Laboratory tests have demonstrated at least a transient effect on creep rate of stress path but its influence in situ is unknown.

6.4.3 Basal Halite

Several closure stations were established along the 1906 drift at the beginning of the programme. The points are from 40m to 200m from the nearest salt stoping and are thus influenced to a varying degree by abutment stresses. While it is clear that proximity to stopes is responsible for higher closure rates at some locations it is not possible to say whether other points are completely uninfluenced. This makes the process of calibrating a model rather difficult.

Having reviewed the field data it was possible to select points for comparison with the models which were at least 120 m away from the stoping operations, with some confidence that they were unaffected by stope abutment stresses. Care was taken to pick points such as station 19 which were in sections of the drift where a plane strain assumption was reasonable. Despite these precautions, stress redistribution or load transfer from mining areas has been reported to occur over large distances in other mines and it may be the cause of some reloading of the monitoring stations.

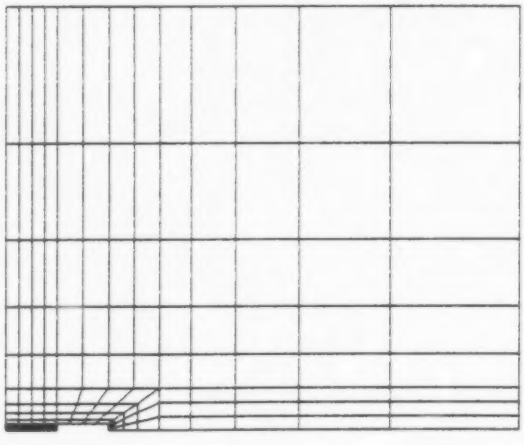

Figure 6.7 Finite element mesh used for main entry drift simulations

The finite element mesh shown in Figure 6.7 was used for the main entry simulations. The lower and left boundaries, which have only perpedicular restraint, act as axes of symmetry to simulate two drifts divided by a 24 m pillar. The material parameters given in Chapter 5 were used for all the Basal Halite simulations.

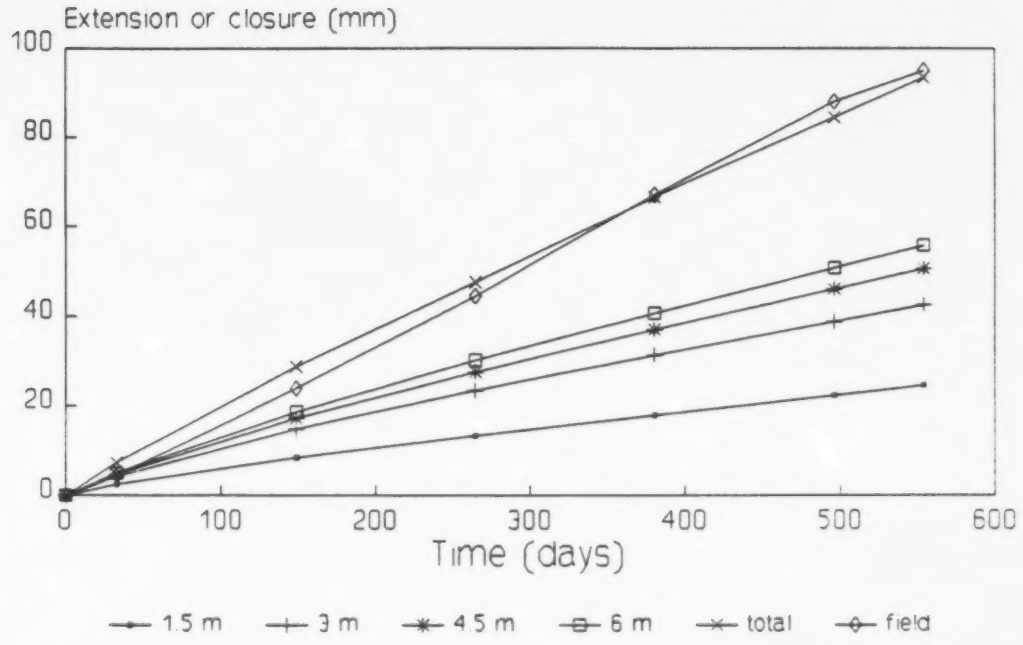

Figure 6.8 Total measured closures compared to closure and wall expansion predictions using the power law

Both the single stage and bilinear laws gave good fits to the steady state closure data from stations in the main entry. Figures 6.8 and 6.9 compare predicted total closure and extensomter extensions to measured total closure. The bilinear law contains a transient which was missed in the field data and that causes an overestimate of total closure. Extensometer data was matched well once steady state had been achieved. The bilinear law slightly overestimates the proportion of total closure occurring in the first 6 m of the wall and underestimates the ratio between expansions of the first 1.5 m and 6 m. The single stage law matches the expansion of the first 6 m closely but also underestimates the proportion of the expansion which occurs in the first 1.5 (50% as compared to 65% from the field results). Possible reasons for this were discussed in the previous section.

Closure rates at stations where there is abutment loading from adjacent stopes can be fitted by raising the effective overburden pressure on the model. The interaction of these abutment stresses is too complex to analyze without the aid of a 3-dimensional visco-elastic model, thus the effective overburden pressure can only be approximated. For instance, to match the closure rates at station 16 it is necessary to raise the overburden pressures by 30% or 4 MPa. While this is reasonable, given the extraction ratio at that location, it is not justified to consider such a fit as model validation.

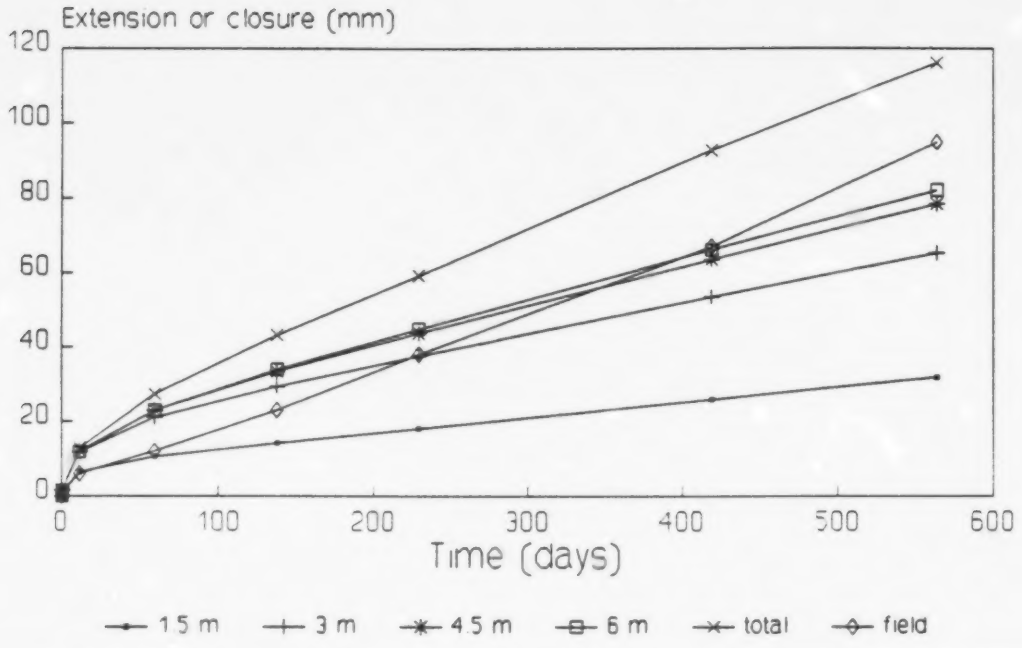

Figure 6.9 Measured closures compared to total closures and wall expansions predicted by the bilinear law

6.4.4 Potash

Suitable entries for instrumenting and modelling were more difficult to obtain in potash than in any of the other strata. Mining within the ore body normally results in complete extraction of the potash on a horizontal plane and the behaviour of the resulting excavation is controlled by potash in the back and floor and salt in the walls. The first excavation discussed here is the 189+00 cross-cut on the 1850 exploration level. It is a 6 m x 3 m entry cut perpendicular to the strike of the ore in an area of very thick ore. This is not ideal for model calibration purposes because the entry length of the entry which is within potash is only 30 m and it is cut from a drift 15 m wide. Thus the cross cut cannot be assumed to be a virgin ground excavation. A ramp was cut 12 m below the cross-cut only 90 days after monitoring had started, further complicating the response of the rock mass.

The mesh used for simulations of the 189+00 cross-cut is shown in Figure 6.10. The lower opening was excavated by removing elements and zeroing normal stresses on the excavated faces 90 days after the start of the simulation.

Laboratory tests indicated a gradually increasing exponent of stress in the constitutive

law. In the stress range used in the tests the exponent on stress was calculated as 8.5 but it is apparant that it must drop rapidly at shear stress values below 8.5 MPa. An exponent of 6 had been used for the bilinear creep law before the laboratory tests were completed and this value has been maintained, in part because it is in better agreement with literature values and in part because extemely high exponents can cause numerical instability in the models. For the power or WIPP steady state laws an exponent of 2 was used with good results. Except for differences in the rate of transient closure immediately after mining, the single stage and bilinear models give similar results. The reason for close agreement between laws with widely different exponents is that the higher exponent in the bilinear law affects only very small volumes of rock close to the excavation boundary.

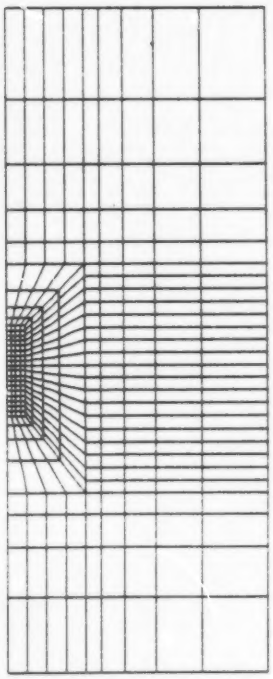

Figure 6.10 Finite element mesh used for simulation of 189+00 cross cut

Predicted and actual horizontal closures in the cross-cut are compared in Figure 6.11. The comparison is remarkably good although there is some deviation at the time of the second excavation. The long period between field readings at this time may have masked the elastic response to the excavation. A contributing factor may also be the delay in elastic response observed in laboratory samples, in which the instantaneous (sonic) modulus is three to four times the tangent modulus measured from core samples. The lower value of modulus has been used for modelling, thus combining both the true elastic and delayed elastic deformations. In the field this delayed elastic response can take several days.

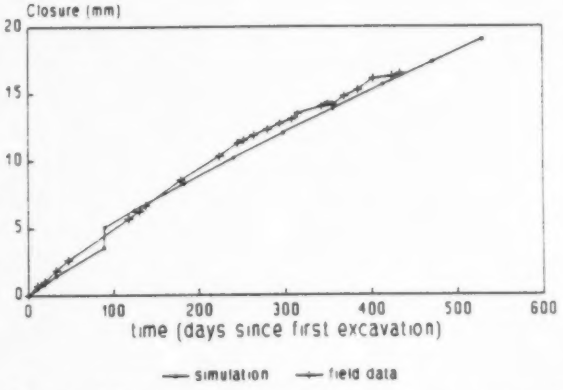

Figure 6.11 Comparison of predicted and measured closures in potash in the 189+00 cross cut

It is common for the influence of an excavation to be greater than predicted by a model, an effect which has been observed both in Saskatchewan and elsewhere in this mine. It

is usually in highly stressed locations that this occurs and it is probably explained by a period of plastic failure immediately following mining which gives way to viscous deformations once elasto-plastic equilibrium has been reached. In the lightly stressed location considered here the response is modelled well by a single component power law since the stress changed resulting from the second excavation is insufficient to cause either plastic deformation or initiate a higher rate creep mechanism.

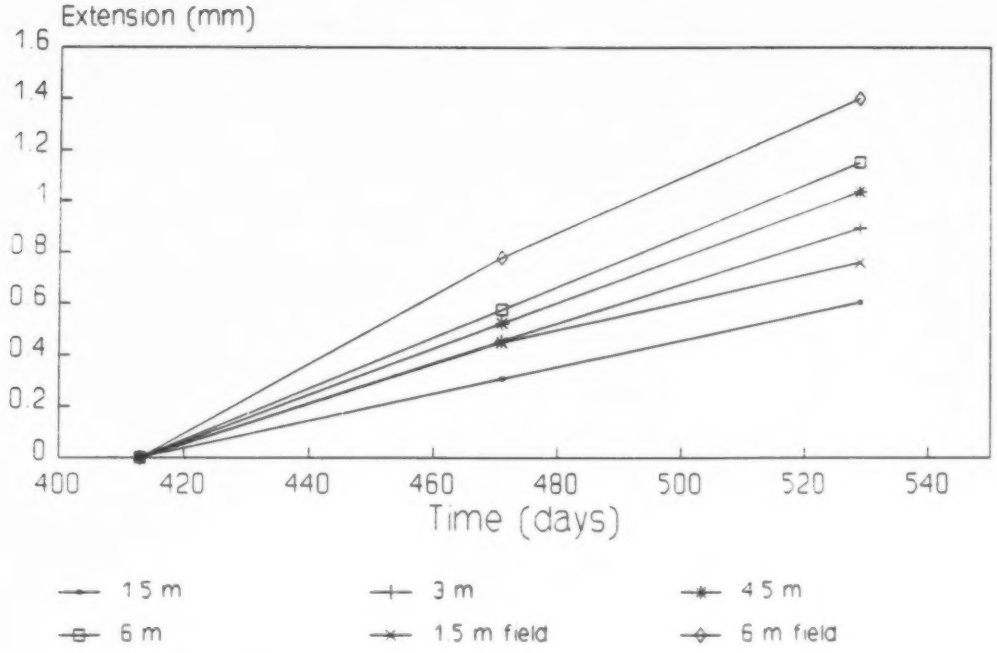

Figure 6.12 Comparison of measured and predicted wall expansions in 189+00 cross cut

Results from wall mounted extensometers were compared with predictions using several stress exponents in the chosen constitutive laws. Increasing the stress exponent has the effect of limiting deformations to a smaller region close to the excavation. For instance, an exponent change from 1 to 6 increases the proportion of the total closure resulting from deformations in the 7 m region closest to the excavation from 86% to 97%. Lower exponents produce a slightly greater extension in the 1.5 m nearest the wall. The best fit to extensometer data was achieved with a stress exponent of 2.0, the results for which are shown in Figure 6.12. 92% of the excavation closure resulted from deformations in the first 6 m of the wall which matched field results. Field measurements of 1.5 m and 6 m extensometers are superimposed on the predicted values in Figure 6.12 and these indicate that although relative extensions are predicted reasonably well, there is an underestimate of about 20% in their magnitude.

6.5 Large scale mine modelling.

Obviously the models which have been developed are of no practical use if they can only be used to design small drifts. The exercise of comparing model simulations to the performance of a series of simple excavations is simply preparation for the real task of analyzing problems too complex for empirical simplifications. The realistic problems are orders of magnitude larger than those used for model calibration and simulations can only be validated by limited measurements in the field. Potash and salt stopes which were monitored for this purpose have been discussed in Chapter 4.

6.5.1 Potash stopes

The central section of the 1900-2 stope has been instrumented most extensively for the purpose of model validation. Closure rates on the mining level of the stope have been recorded throughout its life and extensometers and earth pressure cells have been placed at selected locations. While this information is insufficient to provide a complete picture of the rock mass behaviour it is adequate to provide qualitative validation of the computer model. Assumptions have been made regarding the properties of the backfill, which has not yet been studied in the laboratory. Earth pressure cells in the backfill provide an indication of whether these assumptions are reasonable.

Models of the 1900-2 stope were created with both GEROC and FLAC. They are shown in Figures 6.13 and 6.14. The FLAC model contains more detailed geometry because of the greater number of elements which can be used within the constraints of computer memory capacity. However, the two are capable of a similar level of numerical accuracy.

In both models the mined cavity was modelled as being full of tailings although the interior elements have been removed from the Figures for clarity. In the GEOROC model the non-linear constitutive law described in chapter 5 was used. In FLAC a similar law is not available and the fill was modelled as a Mohr-Coulomb material with constant stiffness (K = 41 MPa, G = 54 MPa). Only two stages of excavation were simulated, one for the first seven lifts of the stope and one for the eighth lift.

Results from the FLAC model (Fig. 6.15) show that the footwall is relieved of stress by the fold in the ore, which explains the very low deformations recorded by the 4th lift extensometer. High stress concentrations naturally exist in the stope back but yielding or very rapid creep relieves stresses near the face and produces safe mining conditions for the life of the lift. The stabilty of the back is only a short term situation and it is probable

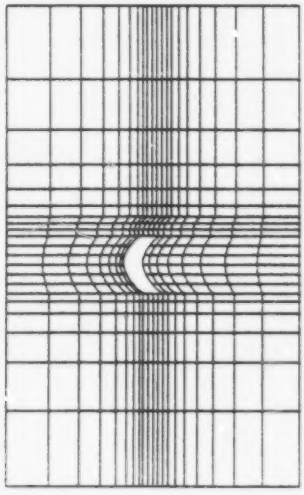

Figure 6.13 Finite element mesh used for 1900-2 stope simulation

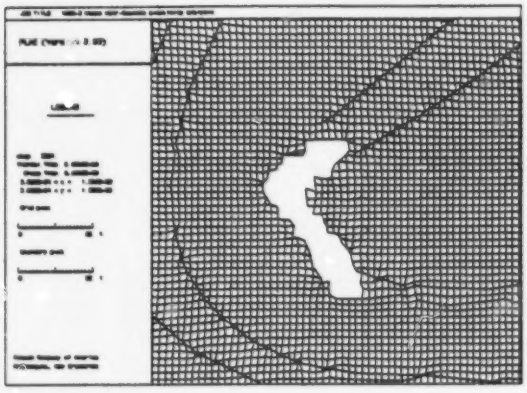

Figure 6.14 Detail of the FLAC mesh used for 1900-2 stope simulation

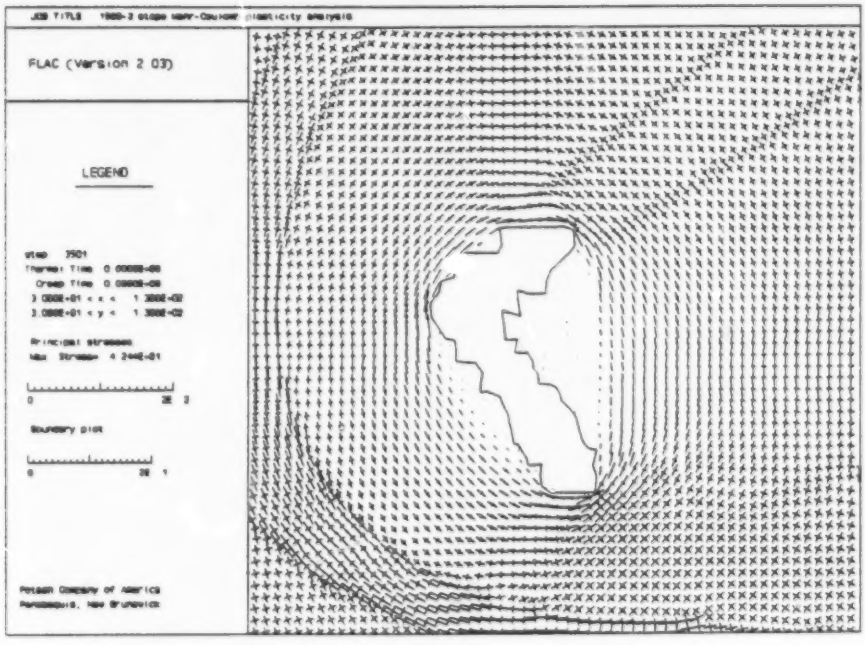

Figure 6.15 Principal stress vectors from FLAC simulation

that creep would eventually lead to the formation of shear fractures and the release of slabs of destressed rock. Six months to one year is the anticipated time before failure of most stope backs. Although it has not yet been done, it should be possible to establish strain or strain rate limits for the occurence of back failures by comparison between models and field performance. Exceptions to the generally sound stope conditions exist where there are slickensided fractures or bedding planes within the ore. In these cases stress relief can take the form of slippage rather than creep and block failures may occur as dictated by the excavation geometry. The no-tension FLAC model correctly predicted the failure of the reentrant corners near the top of the hanging wall where fracturing exists along the bedding planes.

The GEOROC model gave acceptable agreement with field instrumentation despite its relatively crude approximation to the stope geometry. Hanging wall and footwall expansions follow the general trend of the extensometers. As shown in Figure 6.16 the footwall is contracting in the first 9 m due to creep of the convex wall. The expansion at depths of 9 m to 15 m into the wall is overestimated by the model. This is probably explained by the greater degree of folding, and thus greater volume of destressed rock, found in the ore body. The hanging wall expansions (Figure 6.17) decay with distance from the stope at a greater rate than found in situ which may also be a geometrical effect but perhaps indicates that the hanging wall becomes cracked parallel to the face to a depth of 15 m or more. The discrepancy between the field measurements and the predictions is not great enough to indicate that the contribution of non-viscous mechanisms to deformation is significant.

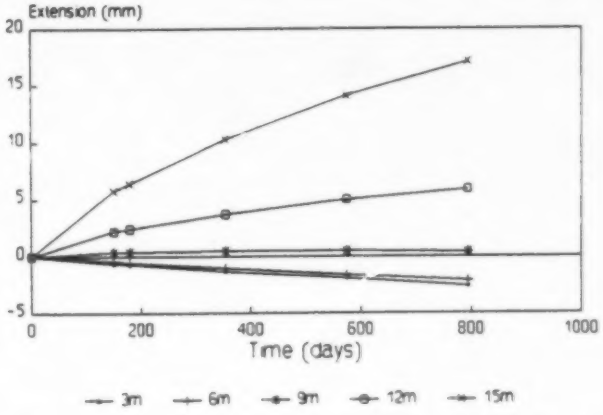

Figure 6.16 Footwall expansions predicted by GEOROC simulation

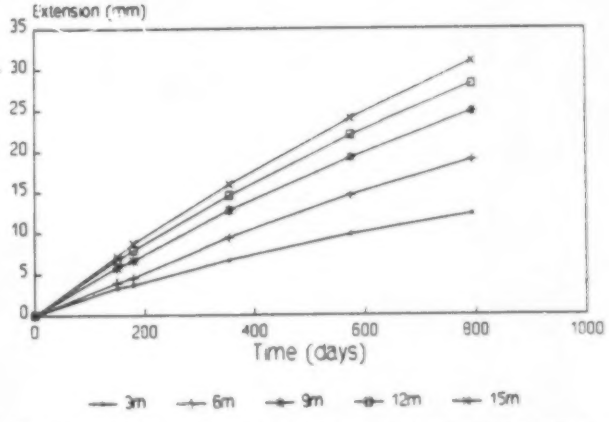

Figure 6.17 Hanging wall extensions predicted by GEOROC simulation

The fill pressure measured to date is below that predicted by both the models. Typically the models overestimate by 100%; the probable

reasons for this were discussed in Chapter 4. In the long term the predicted values are believed to be realistic. In a perfectly filled stope the backfill would take 50% of the overburden load over a period of 5 to 10 years. If the stope is incompletely filled the transfer of load will be much slower, particularly if caving of the hanging wall occurs.

6.5.2 Salt stopes

Rock mechanics considerations are an important aspect of the design of the salt stoping level. The often conflicting goals of optimization of the extraction ratio and protection of the 1900 level main entries can both be achieved if accurate predictive modelling can be performed.

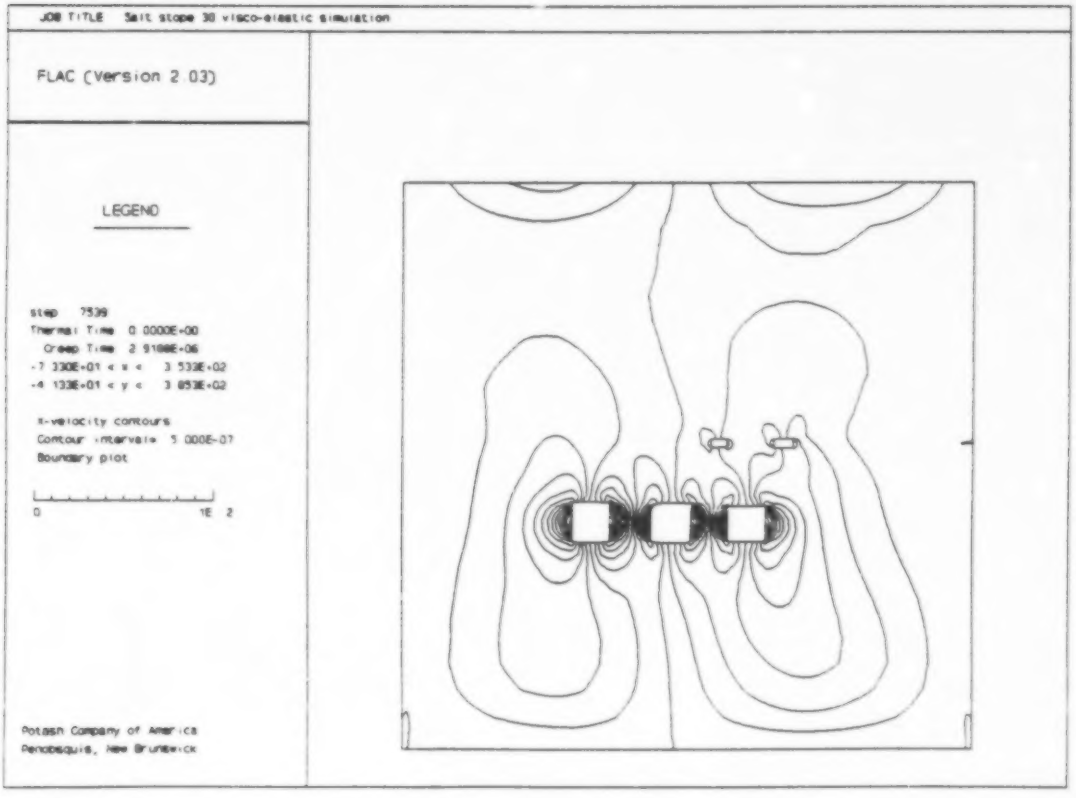

Figure 6.18 Horizontal closure velocities around salt stope 30

The second practical validation exercise carried out with the calibrated models involves a simulation of Salt Stope 30. The stope has three 23 m wide by 18 m high caverns separated from each other by 18 m thick pillars. The back of the stopes are 24 m below the floor of the 1900 level main entry. An assessment of the effects of mining the stope directly beneath the 1904 drift was made prior to mining. This was an important consideration since the drift has been observed to close at excessive rates when using other stope layouts.

A FLAC model was created with 100 elements on the horizontal axis and 50 elements vertically. The lower boundary was fixed, the sides were horizontally restrained and the top left free. Loads were applied to the top to simulate overburden load and hydrostatic in situ stresses were imposed with a gradient equal to the salt self weight. These boundary conditions were used for all large visco-elastic simulations with both FLAC and GEOROC. It has been observed that fixing the top of the mesh always results in destressing of the top boundary as pillar yielding takes place irrespective of the vertical size of the mesh.

Using the creep properties for Basal Halite established in section 6.4.3 a steady state creep analysis of the stope was performed. The primary criterion for concluding the adequacy of the design was the closure rate of the main entries. A maximum rate of horizontal closure of 0.25 mm per day has been found acceptable in practice, while the 'virgin ground' closure rate of the entries is approximately .125 mm per day. Figure 6.18 shows contours of steady state strain rate. A maximum rate of .14 mm per day was predicted in the 1904 drift and a rate of .17 mm per day was predicted in the 1906 drift. An equivalent analysis was run without the stopes to check the accuracy of the model in predicting the closure rate of the drifts. A rate of .13 mm per day was predicted.

The closure rate in the centre cavern of the salt stope was also measured to verify the predicted steady state of .65 mm per day.

At the time of writing, the third leg of the salt stope is being mined and closure rates in the 1904 drift have dropped to about 0.2 mm per day following a peak rate of 0.7 mm per day as the mining passed directly below. The previous salt stope, which was positioned 20 m south of the drift with its back at the elevation of the drift floor, is still causing a closure rate of 0.7 mm per day in the 1904 drift.

6.6 Discussion

Numerical modelling for this programme was carried out using a combination of the finite element code, GEOROC, and the finite difference code, FLAC. Both ran on Compaq 386 computers. Elastic boundary element programs were put to limited use analyzing mining profiles. These facilities represent the state-of-the-art in microcomputer-based analysis and were well suited to the task. The beginning of this project coincided with the

introduction of economical 32 bit microcomputers and thus it was essentially the first time that computing power of this scale was available to the small and medium sized mine at a reasonable cost. The fortuitous timing probably resulted in more analyses being performed for this project than have previously been performed on any project of similar magnitude. This is a turning point of sorts in mining rock mechanics because mines will in the future be equipped to perform far more of their own analyses and will benefit greatly from the readiness with which comparisons between reality and the computer model can be made. Modelling is, after all, an iterative process in which the 'right answer' is unlikey to be found at the first try.

The modelling philosophy followed was to begin by simulating the simplest possible excavations. These were long rectangular tunnels as far as possible away from any other mining influence. It was posssible to find examples in each of the major evaporite units in which mining takes place. If there are no other stratigraphic units within 15 m of the tunnel being studied it is reasonable to assume that the behaviour of that tunnel is dependent upon only one rock type. Unless this situation exists it is virtually impossible to verify the correctness of even the simplest constitutive law. Acceptable levels of agreement were achieved between simulations using the chosen power and bilinear power laws and measurements taken in trial openings. Acceptability was defined as a conditin where the model gave results within $\pm 20\%$ of the measured steady state total closure and wall expansion rates. No attempt was made to match the transient creep which follows immediately after excavation although this can be dealt with to some extent by treating it as delayed elastic strain and adjusting the elastic parameters accordingly. Other approaches are quite feasible but were considered to be unnecessarily complex at this stage. In most of the trial openings the rapid transient creep was comparatively unimportant.

The single stage power law and the bilinear power law each gave the better results in particular circumstances. In general the power law gave better fits to extensometer data, indicating that a stress exponent of around 2 was reasonable for most materials at low shear stresses. However, the bilinear law has apparent advantages in the Basal Halite in which the transition to a faster rate creep mechanism takes place at relatively low stress. The observable slow decay in closure rate throughout the two years over which monitoring took place was better simulated by the bilinear law. Further work to define the coefficients for the bilinear law with an exponent of 2 for stresses below the critical stress would be worthwhile. This may necessitate a reformulation of the bilinear law in GEOROC. While these laws clearly have shortcomings, they give a reasonable balance of accuracy and simplicity, suggesting that a major effort to develop better mechanistic laws for mining work is unwarranted.

Models verified by simulations of trial excavations were further tested on full scale stopes in Potash and Basal Halite. Again, acceptable degrees of accuracy were obtained in comparison to the limited in situ monitoring which was undertaken. In the potash stopes

the modelling was able to provide a plausible interpretation of wall extensometer readings and gave a reasonable match to fill pressure data. FLAC models gave good predictions of short term hanging wall stability and bed separations. The shortcomings, although not well defined, are almost certainly in the prediction of transient creep in the brow following mining and long term, creep induced failure (often called stress relief failure). The ability to correctly predict the relationship between stress, strain and strain rate causing this type of failure would be a clear advantage when designing openings for long term service. For the purposes of stope design, in which long term access is not an issue, the capability of the bilinear law to model the initial high creep rate following mining, and thus estimate the stress transfer ahead of the face, provides an adequate simulation.

In the case of salt stoping, design for long term performance is essential. The main entries, in particular, must remain stable for many years without rehabilitation. Verification simulations performed for salt stopes 29 and 30 yielded good results although at present it is not possible to interpret them reliably in terms of long term stability. This is another instance in which it would be of great benefit to be able to better predict creep induced shearing and delamination of the stope and drift walls.

In summary, the available computer codes allow the construction of numerical models which give an adequate capability for performance matching and design. However, there are still shortcomings in the areas of transient creep and failure prediction which warrant further work. An improved model is also needed for backfill, although this is probably within reach given the existing base of laboratory testing and field data available. The increasing power of computers will undoubtedly make new methods of analysis possible and the trend should be towards using this power for 3-dimensional models rather than unnecessary sophistication in the constitutive laws used in current 2-dimensional codes.

7. Discussion and Conclusions

The long term goal when introducing a rock mechanics programme to PCA was to develop rational methods of excavation design, the application of which would ensure safe and economical mining practices. It was intended that the first phase of the work, reported here, should result in a solid understanding of the basic parameters which govern rock mass behaviour during and following mining. This aim has been achieved and a foundation, upon which future rock mechanics work at the mine can be built, now exists. In addition to this important background information, the programme has already provided the capability for accurate analyses of planned stope layouts and the solution to several practical ground control problems. Of equal importance, it has resulted in the identification of crucial areas for further study.

It was apparent from the outset that the unusual ore body and novel mining method presented unique rock mechanics problems, and that the complete lack of field and laboratory data on the rock mass greatly impeded their solution. Obtaining information on the response of the rock mass to mining and the properties of the intact material was essential. It was unrealistic, though, to expect that sufficient data could be gathered to allow the derivation of reliable empirical design procedures. Numerical modelling, supported by laboratory testing and selectively verified by field measurements, was identified as the procedure which would most quickly yield a capability for design. Empirical guidelines, which are often more useful for routine design than sophisticated numerical models, can be foreseen as the end product of this integrated approach, just as they are of the observational approach traditionally used at other potash mines.

Elastic and visco-elastic properties of the evaporite rocks in the mining horizon were shown by laboratory tests to be similar to those of other similar rocks described in the literature, excepting a rather low average Young's modulus of 6.5 GPa. This low value cannot readily be explained in terms of sample damage or testing procedures and it does compare well with observations of rock mass performance. Unconfined compressive strengths were in the range of 19 to 26 MPa which is typical for evaporites. The failure strength envelopes obtained from triaxial tests show the expected, strong non-linearity. Failure could not be initiated at confining stresses greater than 3 MPa because of the high strain rates required. Mohr-Coulomb, Hoek-Brown and Rothenburg failure envelopes were derived. The Mohr-Coulomb criterion was employed for visco-plastic analyses although there are serious limitations to a linear envelope. The two non-linear envelopes give similar results and one is not clearly superior to the other; both are applicable only in the range of stresses used in the tests from which they are derived because the true envelope flattens off dramatically at higher stresses. Although brittle failure cannot be initiated at higher confining stresses the practical distinction between very rapid creep and failure is moot.

A series of multi-stage creep tests were performed on core samples to determine their

steady state creep properties. Linear and bi-linear power laws were fitted to the results. At the hi:h stress levels of the laboratory tests, the power law exponents for the halites were in the commonly quoted range of 4 to 4.5. The potash stress exponent, 8.5, was much higher. Laboratory and field data point towards a lower stress exponent of around 2 for all the rock types at shear stresses below about 6 MPa. The transition point, or critical shear stress, dividing the two portions of the bilinear law apparently varies from 6 MPa to 12.5 MPa for the three evaporites tested. It must be stressed that the critical stress is little more than a numerical convenience since there is no evidence from this study to indicate a sharp transition rather than a gradual increase in stress dependency. In fact a gradual change of exponent has been observed in creep tests on other salts.

In accordance with the strategy adopted for the rock mechanics programme, in situ monitoring was begun in remote exploration drifts which were extremely stable. Although the behaviour of these drifts was of little practical interest, they provided ideal locations for collecting information to verify and calibrate the numerical models. The results of laboratory tests were mirrored by the behaviour of these drifts, with clear distinctions between the slow closure in Upper Halite and the rapid deformations in Basal Halite. The order of magnitude difference in moisture content of the two salts is the most likely reason for this difference, although the high purity of the Basal Halite may also be significant. Deformation of the Potash and Middle Halite was at an intermediate rate.

A cut-and-fill potash stope was instrumented at two levels with extensometers and earth pressure cells. While the instrumentation at the upper level has only been operational for a short time, that at the lower level has given much useful data. The fill was shown to arch between the walls after only a few lifts (13 to 15 m) had been placed and vertical pressures did not increase further. The gaps left beneath overhanging walls was found to cause periodic slumping and shrinking of the fill and pressure beneath the overhang built up in an erratic, cyclical manner. Pressures were well below the calculated hydrostatic head and it is projected that the fill will not take more than 5% of the in situ rock stress within the stope life. Extensometers indicated that deformations, perhaps including small fractures or bed separations, extend well beyond the 15 m distance from the walls for which data is currently available. The new level of instrumentation includes 30 m extensometers.

Computer programs for the numerical modelling work were chosen carefully, based upon their features and capabilities and upon their ease of use. The programs are expected to be a part of the mine design process for the next several years and it was important that they could be used by non-specialists. This meant a certain amount of trial and error, trying, and sometimes rejecting, programs that looked promising. Computer models using the chosen finite element and finite difference programs were first verified against measurements from the exploration drifts. Using laboratory defined exponents in the power laws, the stress coefficients were determined by fitting field data. It was not possible to make the assumptions about stress distribution in the drift walls which would

have allowed a direct determination of these coefficients.

Once the material parameters were fitted with acceptable accuracy, several models of stopes were analyzed. The results were compared to data gathered in those stopes. Deformations were predicted with better than 30% accuracy and matching relative displacements and expansions of the walls was extremely encouraging. The analyses assisted considerably in the interpretation of stope behaviour, which was unclear from the instruments because of the narrow coverage they provided. Hanging wall slabbing in the 1900-2 stope was predicted with accuracy, indicating the ability of the models to provide useful assessments of local and global stability. Modelling has now reached the stage at which design work can be carried out with confidence and several projects are being undertaken in which designs will be checked by field monitoring. The implications of refining stope and ramp designs using accurate analysis are considerable and the effort expended on the rock mechanics programme will be thoroughly justified if the design efforts are successful.

Rock mechanics requirements for the future may be divided into groups. The first group comprises all the routine work which should be continued if the gains of the past two years are not to be lost. The closure rates of selected drifts and all potash stopes must be monitored, along with the 1900-2 stope buried instrumentation. Analyses should be run on all new stopes and ramp/stope layouts in an attempt to optimize stope stability and reduce ramp maintenance. Analyses should always be confirmed by field monitoring during and after construction in order that the computer models can be continuously checked and refined. Safety related monitoring of the expansion of drift backs should be continued in order to give reasonable advance warning of ramp rehabilitation requirements. Borehole closure measurements should be continued to supplement the in situ stress data and to confirm the relationship between depth (stress) and strain rates. This information will further validate the evaporite constitutive laws. It is essential to have it if the feasibility of mining at lower levels is ever to be assessed quantitatively. Lastly, an effort should be made to install pressure cells in a crown pillar to ascertain the load bearing capacity of 12 m pillars.

The second group comprises individually funded or new initiatives. Two valuable projects are currently underway. The first is the monitoring of surface subsidence. The relationship between underground closure and surface subsidence is a vital one since it is indicative of the strain energy building up in the overburden and the degree of fracturing being induced. These factors have implications for the potential of induced seismicity and the stability of the mine workings. Early detection of anomalies in surface subsidence will allow timely changes in mine design to be made. The second project is one to develop instruments for fill consolidation measurements, employing radio frequency remote data acquisition. The stope layout employed at PCA makes the use of cabled instruments difficult and expensive. Wireless data acquisition will reduce the cost and delays associated with cable damage. This development provides the means to undertake a third essential

programme, an assessment of in situ backfill characteristics and methods of improving initial fill placement. Much of the success of mining in the future will depend upon high quality backfill. The mine has not yet reached a critical extracted area (one in which the full overburden load will eventually be carried by backfill), but it is probable that once the currently active stopes have been completed the extracted area will be supercritical for the remaining life of the mine. Hanging wall loads must be transferred to the fill with minimal caving if long term, total extraction mining is to be a achieved safely.

8. Acknowledgememts

Funding for this project was provided jointly by New Brunswick Department of Natural Resources and Energy and Potash Company of America, Division of Rio Algom Ltd. The support of both organizations is gratefully acknowledged. Individuals whose advice and encouragement during the course of the work has been welcomed are Dr. G. Herget of CANMET, Mr. A.D. Mackintosh of Cominco Ltd. and Dr. E. Hoek of the University of Toronto. The formal technical review provided by the latter was most helpful.

9. References

Baar, C.A. 1977. *Applied salt rock mechanics I: the in situ behaviour of rock salts.* Elsevier Scientific Publishing Company, Amsterdam.

Baleshta, J.R. & M.B.Dusseault 1988. Triaxial testing of intact salt rocks: pressure control, pressure systems, cell and frame design. In R.T. Donaghe, R.C. Chaney & M.L. Silver, Eds., *Advanced triaxial testing of soil and rock, ASTM STP 977,* American Society for Testing Materials, Philidelphia, pp. 155-168.

Beddoes, R.J. 1984. *Determination of engineering properties of waste salt for backfilling in underground potash mines.* CANMET project no. 310104 RE/SPEC Ltd., Calgary.

Brady, B.G.H. & E.T.Brown 1985. *Rock mechanics for underground mining.* George Allen & Unwin Ltd., London.

Cominco 1987. *Prediction and monitoring of excavation behaviour.* Report to CANMET for contract no. OSQ85-00211 Cominco Fertilizers, Vanscoy, Sask.

Dawson, D.E. 1979. *Preliminary deformation-mechanism map for salt (with application to WIPP).* SAND-79-0076. Sandia National Laboratories, Albuquerque.

Day, R.L. 1985. *Analysis of creep in concrete by rate and activation-spectrum theories.* University of Calgary research report No. CE85-4

Denison-Potacan Potash Company 1987. *Use of backfill in New Brunswick potash mines.* Report to CANMET for contract no. OSQ85-00208 Denison-Potacan, Sussex, N.B.

Dusseault M.B., L.Rothenburg and D.Z.Mraz 1987. The design of openings in salt using a multiple mechanism viscoplastic law. *Proceedings of the 28th Symposium on Rock Mechanics.* Tucson, Arizona. pp. 633-642.

Dusseault, M.B., D.Mraz, J.Unrau & C.Fordham 1985. Test procedures for salt rock. In E. Ashworth, Ed., *Proceedings of the 26th Symposium on Rock Mechanics.* Rapid City, S.D. pp. 313-319.

Fossum, A.F., R.R.Brander, J.D.Chieslar & H.Y.Tammemagi 1985. *GEOROC: a numerical modelling package for designing underground openings in potash.* Report to CANMET for contract no. OSQ83-00269 RE/SPEC Ltd., Calgary.

Fordham, C. & M.B.Dusseault 1988,1989. *Creep and brittle yield testing of intact salt rocks from the Potash Company of America potash mine, Sussex, New Brunswick.* University of Waterloo.

Hesterman, L. 1979. *A brief study of compaction and water expulsion in compressed potash mine tailings.* Report No. E79-8 Saskatchewan Research Council, Saskatoon.

Hoek E. & E.T.Brown 1980. *Underground excavations in rock.* Institution of Mining and Metallurgy, London.

Holcomb, D.J. & D.W.Hannum 1982. *Consolidation of crushed salt backfill under conditions appropriate to the WIPP facility.* SAND-82-0630 Sandia National Laboratories., Albuquerque.

Itasca 1988. *FLAC: Fast Lagrangian analysis of continua.* Computer program users manual. Itasca Consulting Group, Inc., Minneapolis.

Kappei, G. & K.Gessler 1984. In situ tests on the behaviour of backfill materials. In H.R.Hardy & M.Langer Eds., *The mechanical behaviour of salt II.* Trans Tech Publ., Clausthal-Zellerfeld.

Korthaus, E. 1984. Effect of backfill material on cavity closure. In H.R.Hardy & M.Langer Eds., *The mechanical behaviour of salt II.* Trans Tech Publ.,Clausthal-Zellerfeld.

Miller, H.D.S. 1983. Use of rocksalt as backfill. In R.M.McKercher Ed., *Potash technology.* Saskatoon, pp. 341-345.

Pfeifle, T.W., P.E.Senseny & K.D.Mellegard 1984. *Influence of variables on the consolidation and unconfined compressive strength of crushed salt.* RSI-260 RE/SPEC Inc.,Rapid City, S.D.

Reischbieter, F. 1984. Stress distribution and flow in salt domes. In H.R.Hardy & M.Langer Eds., *The mechanical behaviour of salt II.* Trans Tech Publ., Clausthal-Zellerfeld.

Starfield, A.M. & P.A.Cundall 1988. Towards a Methodology for Rock Mechanics Modelling. *Int. J. Rock Mech. Min. Sci. & Geomech. Abstr. Vol. 25, No. 3,* pp. 99-106.